

Evolution of Developmental Control Mechanisms

The embryonic development of the centipede *Strigamia maritima*

Carlo Brena*, Michael Akam

Laboratory for Development and Evolution, Department of Zoology, University of Cambridge, Downing Street, Cambridge CB2 3EJ, UK

ARTICLE INFO

Article history:

Received for publication 28 July 2011

Revised 18 October 2011

Accepted 10 November 2011

Available online 19 November 2011

Keywords:

Chilopod

Segmentation

Developmental rate

Staging

Arthropod

Geophilomorpha

ABSTRACT

The geophilomorph centipede *Strigamia maritima* is an emerging model for studies of development and evolution among the myriapods. A draft genome sequence has recently been completed, making it also an important reference for comparative genomics, and for studies of myriapod physiology more generally. Here we present the first detailed description of myriapod development using modern techniques. We describe a timeline for embryonic development, with a detailed staging system based on photographs of live eggs and fixed embryos. We show that the early, cleavage and nuclear migration, stages of development are remarkably prolonged, accounting for nearly half of the total developmental period (approx 22 of 48 days at 13 °C). Towards the end of this period, cleavage cells migrate to the egg periphery to generate a uniform blastoderm. Asymmetry quickly becomes apparent as cells in the anterior half of the egg condense ventrally to form the presumptive head. Five anterior segments, the mandibular to the first leg-bearing segment (1st LBS) become clearly visible through the chorion almost simultaneously. Then, after a short pause, the next 35 leg-bearing segments appear at a uniform rate of 1 segment every 3.2 h (at 13 °C). Segment addition then slows to a halt with 40–45 LBS, shortly before the dramatic movements of germ band flexure, when the left and right halves of the embryo separate and the embryo folds deeply into the yolk. After flexure, segment morphogenesis and organogenesis proceed for a further 10 days, before the egg hatches. The last few leg-bearing segments are added during this period, much more slowly, at a rate of 1–2 segments/day. The last leg-bearing segment is fully defined only after apolysis of the embryonic cuticle, so that at hatching the embryo displays the final adult number of leg-bearing segments (typically 47–49 in our population).

© 2011 Elsevier Inc. All rights reserved.

Introduction

“The myriapods yield up their embryological secrets only as a reward of great patience, ingenuity and histological skills.” (Anderson, 1973)

Myriapods are now recognised as an ancient clade among the arthropods, but despite the large number of studies of arthropod development in recent years, we still know very little about their development. Yet if we are concerned to understand the diversity of developmental mechanisms among the arthropods, and how these mechanisms may have evolved, then it is essential to sample all of the major extant lineages within this diverse group.

Myriapods are specifically interesting in that they constitute a basal branch of the mandibulate arthropods that has retained a relatively simple, and possibly ancestral, body plan with only limited trunk segment diversity. They are an appropriate outgroup for comparison with the diversity of all insects and crustaceans, and may retain developmental mechanisms that have been modified or overwritten in these better-studied clades.

There are two major groups of myriapods—the grazing millipedes, which have two pairs of legs on most trunk segments, and the carnivorous centipedes, which are uniquely characterised by the transformation of the first trunk segment into a venomous poison claw or forcipule. In this paper, we provide the first detailed modern description of embryonic development in a centipede, using as our model *Strigamia maritima*, the only myriapod for which a complete genome sequence is now available.

The order of centipedes to which *Strigamia* belongs, the Geophilomorpha, is exceptional in that adult segment number is established at hatching, but is highly variable, both between species and within populations. This makes it particularly amenable for studies both of the mechanisms of segmentation (Chipman and Akam, 2008; Chipman et al., 2004a), and of the factors underlying variation in final segment number. In *Strigamia*, these factors include both environmental temperature during embryogenesis (Vedel et al., 2008, 2010), and genetic factors (Vedel et al., 2009).

The list of publications on the embryonic development of centipedes is not long. From the nineteenth century on, these are: (organised by order, from more basal to more derived) Scutigermorphs (Dohle, 1970; Knoll, 1974), Lithobiomorphs (Hertzel, 1983, 1984; Kadner and Stollewerk, 2004), Scolopendromorphs (Dawydoff, 1956; Heymons, 1898, 1901; Ivanov, 1940; Sakuma and Machida, 2002,

* Corresponding author.

E-mail addresses: cb508@cam.ac.uk (C. Brena), m.akam@zoo.cam.ac.uk (M. Akam).

2003, 2004, 2005; Whittington et al., 1991) and Geophilomorphs (Chipman et al., 2004b; Metschnikoff, 1875; Sograff, 1882, 1883).

Only three of these studies provide detailed descriptions of centipede development from the very early stages (Heymons, 1901; Knoll, 1974; Sograff, 1883), and none provides a timeline for development. All major reviews on centipede development, and indeed of myriapods as a whole, have been based exclusively on Heymons' description of *Scolopendra* (Anderson, 1973; Gilbert, 1997; Johannsen and Butt, 1941).

Both Heymons' description of *Scolopendra*, and Sograff's description of a geophilomorph similar to *Strigamia* are excellent detailed studies, but both are limited by the tools of the nineteenth century, and indeed by the preconceptions of their authors. One significant error in Heymon's description has already been pointed out by Chipman et al. (2004b). (Heymon inverted the orientation of the AP axis at early germ band stages, which led him to the incorrect inference that the most anterior segments form in a posterior to anterior direction). A modern description is clearly needed to form the basis for more specific studies of all aspects of myriapod development.

We have previously published a brief description of *Strigamia* development (Chipman et al., 2004b). At that time, it was thought that the eggs of these centipedes would not survive for long when removed from the care of the mothers, but we have found this not to be true. We can now rear them reliably from the earliest stages to hatching, and beyond. This has allowed us to determine a timeline for development under standard conditions, and to provide a far more detailed description of development from sequential and time-lapse observations. This reveals that some assumptions in that earlier work were incorrect (e.g. that segment addition is complete at the time of sinking).

The only other staging series published for centipedes is that published for the scolopendromorph *Ethmostigmus rubripes* (Whittington et al., 1991). However, there are considerable differences in the relative timing of developmental events in scolopendromorphs as compared with geophilomorphs, so the two staging series are not directly comparable.

In defining stages of development, we have considered two main criteria:

- 1) That the stages represent a distinct phase of development, clearly distinguishable from the preceding and following stages.
- 2) That, in so far as possible, the stage should be recognised from the external morphology through the chorion, so as to provide a useful and practical tool to stage and score both live and fixed eggs.

Although much of what we report confirms and extends earlier studies, we also correct some earlier misapprehensions, concerning for example the timing of segment addition, and highlight some unusual aspects of geophilomorph centipede development not previously appreciated.

Materials and methods

Field collection and culturing of eggs

Strigamia maritima eggs were collected from a previously studied population (Chipman et al., 2004b) near Brora (Scotland) in late May or early June across the years 2006 to 2010. Individual clutches of eggs were collected from the brooding females into 6 cm diameter plastic Petri dishes, either on filter papers moistened with Locust Embryo Saline (LES, Ho et al., 1997) or into a shallow layer of mineral oil (Sigma M8410, embryo tested, Vedel et al., 2010). Petri dishes with clutches were placed into closed water saturated boxes within insulated cooled containers and kept between approx 10 and 20 °C until returned to the laboratory (typically 24–36 h after field collection). In the lab, the boxes were kept in incubators set at temperatures

between 8 and 25 °C. We used 13 °C as the standard incubation temperature for the work described here, unless stated otherwise. Some clutches were initially kept at 4 °C, a temperature at which development almost stops. This extended the period of availability of embryos for experimental work.

Potentially gravid females were also collected in the field into small egg lay chambers (2 ml tubes or small boxes with some matrix collected from the egg lay site) and returned to the laboratory, where they were inspected after 2–16 days. A few of these (7/38) laid clutches of eggs in the lab, which were cultured on moist paper as above.

Egg fixation, staining, sectioning and visualisation

Eggs maintained on LES soaked filter papers were fixed in 4% formaldehyde in 0.5X PBS (1–3 days at room temperature), after incubating them for 30 min in 0.5X PBS (to increase turgidity and reduce shrinkage during fixation). Eggs cultured under mineral oil were fixed in 50:50 heptane: 4% formaldehyde in 0.5X PBS, on a nutating mixer for 1–3 days at room temperature. For storage after fixation, eggs were rinsed in PBS, de-hydrated through a PBT:methanol series over 20'–40', and kept in 100% methanol at –20 °C. Eggs were then manually dechorionated using fine tweezers (Dumont 55) and rinsed in PBT (PBS + 0.1% Tween 20). Even after long fixation, it is difficult to dechorionate the earliest stages without damaging the egg surface. The chorion is freely permeable to water and formaldehyde, but not to any of the stains that we have tried (see Results).

Selected dechorionated eggs were stained with nuclear stains—Hoechst 34580 (2 µg/ml), Sybr Green (1X) or Sytox Green (1 µM), and stained for actin with FITC phalloidin (SIGMA, 1 µg/ml), in all cases for 1 h on a shaker at room temperature in PBT.

Pictures of whole eggs (both live and fixed) were taken with a Leica MZFLIII stereomicroscope with a Leica DFC 500 Camera (Leica Firecam software), with lateral light and black background. Pictures of some fixed eggs were taken with a Leica TCS SP5 confocal microscope, immersed in an anti-bleaching medium (85.5% glycerol, 5% DABCO, 9.5% PBS) on a microscope cavity slide with a cover slip.

Selected blastoderm and germ band stage embryos were manually dissected from the yolk with fine tweezers and very fine brushes and flat mounted in 15 µl of 70% glycerol in PBT on a microscope slide with a cover slip.

For sectioning, fixed eggs were dehydrated through a PBT:ethanol series. From 100% ethanol, they were washed in 1:1 100% ethanol:acetone for 15', then in acetone 2X for 15', then overnight in 1:1 acetone:catalysed resin (Araldite 502, 19%, EMBED 812, 24%, DDSA, 57%, Electron Microscopy Sciences), all at room temperature and in sealed containers. Embryos were then placed in 100% resin for around 5 h in open containers, mounted in 100% resin in embedding moulds and left to polymerize for 2 days at 60 °C. Semithin sections were made with an ultramicrotome and stained with toluidine blue.

Pictures of flat mounted preparations and sections were taken with a Zeiss Axiophot compound microscope with a Leica FC3 FX camera. Contrast and colour of the photos were adjusted using Adobe Photoshop.

Chorion thickness was measured on transverse sections of fixed eggs.

Time-lapse microscopy

To follow development directly, eggs were viewed by time lapse microscopy using a Zeiss Axioskop 2 mot plus compound microscope, with an Axiocam MRm camera and Axiovision rel 4.6 software. To mount the egg, a ring of silicone grease (approx 2 cm in diameter and 1.5–2 mm high) was prepared on a glass slide, with an additional small droplet of grease at the centre of the ring to hold the egg in position. The egg was placed on the central droplet, covered with

culturing mineral oil and rotated with a fine brush under the stereomicroscope to reveal the germ band in lateral view. The slide was then mounted on a temperature controlled stage held at 18 °C with a Linkam PE94 heat controller (Linkam scientific instruments, UK). Eggs were illuminated with lateral light from a fibre optic light source on a black background.

Eggs mounted like this at the first sign of head segmentation will generally survive under the microscope for several days (although they are not able to complete dorso-ventral flexure if thus mounted for more than a day—see example Time Lapse 1, TL1, Supplementary material). Unfortunately, although the chorion is held still, the egg tends to rotate inside the chorion, quickly moving the germ band out of view (see for example Time Lapse 0, TLO, Supplementary material).

Of 40 eggs initially stable at the beginning of time lapse observation, only five remained stable long enough to produce useful time lapse movies (Supplementary information, TL1–TL5). Even in these best cases, it has not been possible to identify with precision the addition of single segments to estimate the segmentation rate directly.

Description and timing of development

We have used 2 methods to establish the series of developmental stages, and to estimate the duration of each stage:

- 1) For pre-germ band stages, which do not show any clear morphological staging markers externally, we selected 8 young clutches (including clutches identified as soft white eggs, i.e. very young – see staging –, during field collection), and fixed two eggs from each clutch at regular intervals, generally every 48 h. Eggs within a clutch are sufficiently synchronous (see below) that these samples give a good representation of the stage of the whole clutch, allowing the sequence and duration of these stages to be estimated. The sampled eggs were photographed, then dechorionated or, in the case of the youngest eggs showing no superficial nuclei, cracked open and stained to reveal internal nuclei and general morphology. Some of these eggs were sectioned. Data collected in this way are shown in Fig. 1, and also Figs. 2f, 6e and h.
- 2) For blastoderm and following stages, we selected 8 clutches and fixed two eggs from each clutch to establish the stage of the clutch at the starting point of our observations. We then followed 26 single eggs from these 8 clutches individually, as they developed, photographing each egg every 2 days, and every day for some eggs at particular stages of development. The live eggs shown in Figs. 2–6 were staged in this way.

These observations on live eggs were correlated with those on fixed eggs by selecting eggs on the basis of external appearance, and then fixing and staining these as described above. This allowed us to confirm the extent of blastoderm development, head condensation, etc. corresponding to different external morphologies. These results provided the panels of fixed embryos in Figs. 2–6.

To establish the complete timeline for development, we have incorporated the data from both methods above, together with observations on additional single eggs and clutches, to give a total dataset of 35 individually staged eggs, and 23 clutches followed as units.

Because we do not know the precise time of egg laying for most of our clutches, we need to correlate the staging data from different eggs and clutches in some other way. Wherever possible, we have done this by using as a fixed point a well defined developmental stage, the midpoint of dorso-ventral flexure. This can easily be determined by external observation, and eggs differing by as little as 6 h (<1% of developmental time) can readily be distinguished. Tabulated data for each egg or clutch have been aligned using this reference point, which lies at about 75% of development. For eggs that were fixed (or died) before stage 6, data were aligned by correlating other well defined developmental stages (e.g. the appearance of cells at the

egg periphery (i.e. the soccer ball stage)) or the number of trunk segments.

For the few clutches that were laid by gravid females in the lab, we know both the earliest and latest dates of egg lay, but as females are reluctant to lay eggs when disturbed, we do not know the precise date of egg lay. In two cases, we have followed such clutches to stage 6 or beyond. These observations, made at 11 °C, allow us to define the maximum duration of development, comparing the relative duration of different stages at distinct temperatures, according to the percentage of total development.

The aligned tabulated data were used to estimate the duration of each stage, and the overall duration of development as reported in Fig. 8. The greatest uncertainty pertains to the duration of the earliest cleavage stages, for which we have few observations.

For early stages, cell numbers have been estimated by approximating the central, pre-migrating population of cells to a sphere (for late stage 1.2, 'sphere' radius approx 8–10 cells), and for early blastoderm stage (early stage 2.1) approximating the blastoderm to a spherical surface uniformly populated with cells, and extrapolating from the number of cells along a linear segment of the surface.

Clutch synchrony

The synchrony of eggs within single clutches was estimated in two ways. For 6 clutches fixed in the field during the main phase of trunk segmentation, the number of segments visible in each egg was counted. Knowing the rate of segment addition (see below), we could estimate the age range of eggs in each clutch.

For a further set of clutches, eggs were selected at stage 5, and all eggs of each clutch were observed at least twice daily, until all had undergone dorso-ventral flexure. The extent of "sinking" was recorded for each egg at each time point, and the time of mid-sinking (ingression of the germ band reaching the middle of the egg) estimated for all eggs. These observations were made on eggs cultured at 10–11 °C. This method has the advantage that the dispersion of developmental ages is measured directly at a well defined developmental point, but the disadvantage that laboratory culture, and regular handling for observation, probably increases the asynchrony of eggs within a clutch.

Segment numbers

Segment numbers were counted in live embryos under the dissecting microscope. The 1st leg-bearing segment (1st LBS) was distinguished from the adjacent forcipular segment (the first trunk segment) by its smaller primordium. The last segment to be counted was that defined by both anterior and posterior furrows. Such visual segment counts are only accurate to about +/- one segment. There is some ambiguity in defining the last visible segment.

The final number of leg-bearing segments is variable in *Strigamia maritima*, as in most geophilomorph centipedes, ranging from 43 to 53 in the Brora population (Vedel et al., 2008), with females having on average two more leg-bearing segments than males. Consequently the segment counts used to characterise the stages of segment addition (from stage 4 onwards) are not precise, and in particular apply specifically to the Brora population.

Results

The system: brooding and the egg

In the *Strigamia* population at Brora, egg laying takes place from mid May to early June. Females occupy brood chambers—small cavities in the matrix of sand, silt and earth, typically placed just adjacent to a large embedded pebble, some 10–40 cm beneath the surface of the shingle. The matrix temperature measured at these egg laying sites ranged between 10 and 18 °C in different collection years, but

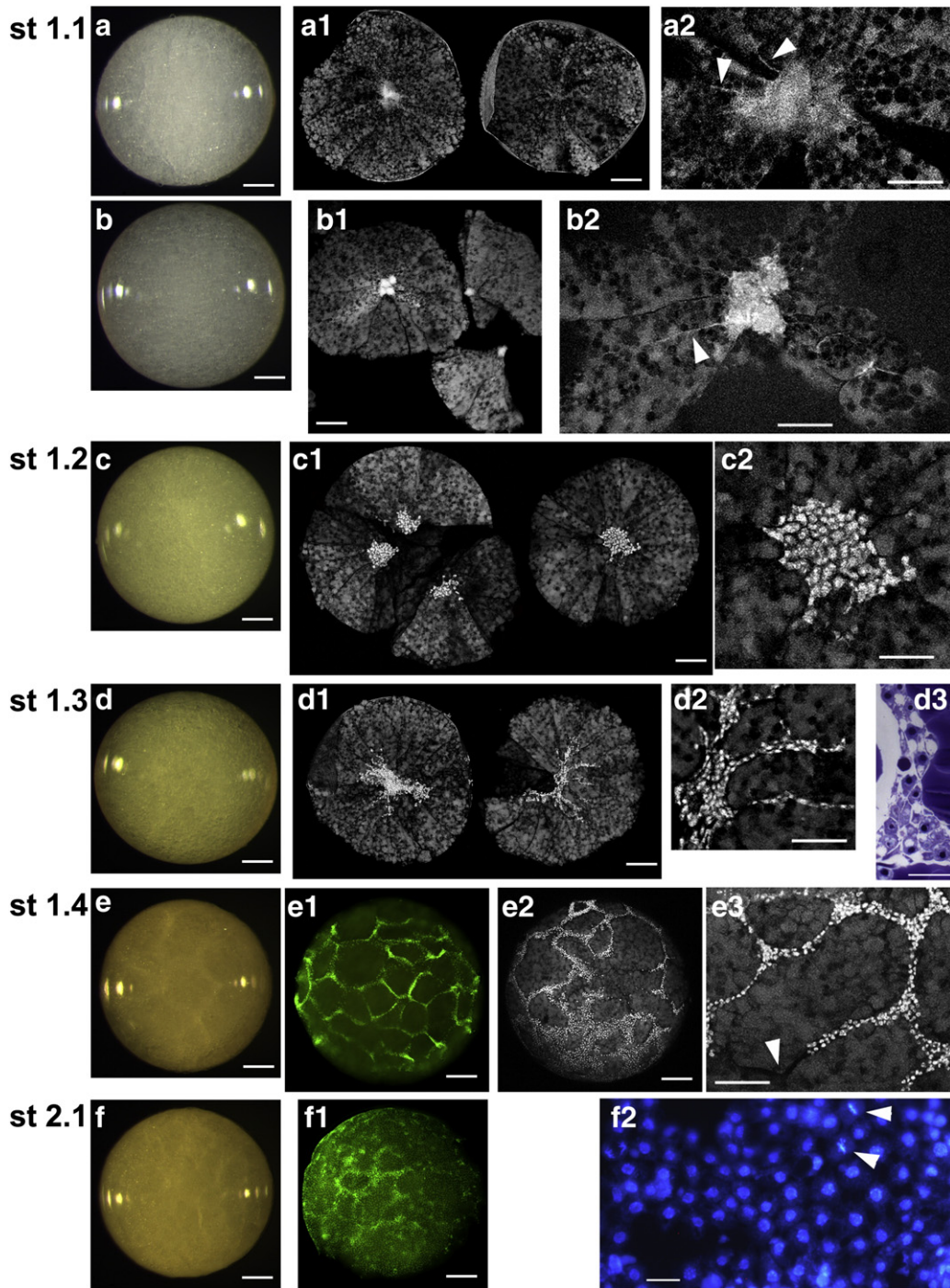


Fig. 1. Developmental stage 1, cleavage and peripheral migration: *Strigamia* eggs (stages 1–2.1) fixed at regular intervals of time from selected clutches, arranged in temporal order (see first method of [Description and timing of development](#)). a, b, c, d, e, respectively approx 4, 6, 10, 18, 20 days after deposition (at 13 °C), f approx as e, but slightly later developmental stage (a–d are eggs from a single clutch). a–a2, b–b2: Stage 1.1: early blastomeres dividing at the centre of the egg, with actin filaments departing centrifugally (arrow heads in a2, and b2). c: Stage 1.2: division at the centre of egg produces a large population of cells. d: Stage 1.3: cells migrating towards the periphery through the inter-pyramidal spaces. e: Stage 1.4: cells reaching the surface of the egg (arrowhead in e3 shows inter-pyramidal split after accidental removal of cells occupying it). f: Early stage 2.1: cells spreading, also through cell division (arrow heads showing mitotic figures in f2), on the surface to form a blastoderm enclosing the whole egg. a–f: View of the whole fixed egg, stereomicroscope; a1–f1, e2 eggs at same stages as a–f (b1 same egg as b); a1–d1, e2 confocal microscopy, maximum projection; e1–f1 stereomicroscope, fluorescent light; a1–d1: eggs opened in two halves to show the centre, e1, e2, f1: superficial view of dechorionated eggs; a2, c2, d2 high magnification of a1, c1, d1; b2 high magnification of b1, but on different emission channel and maximum projection only on few optical sections; e3: high magnification of same egg as e2, but view from different point of view. a1, a2, b2: actin stained with phalloidin FTC; b1: nuclear stained with Hoechst 34580, c1–f1, c2–e2, e3: nuclear stained with Sybr Green. In all these pictures high level of autofluorescence and of background are in fact showing the shape of the yolk and of the overall egg. d3: Section (toluidine blue stained) of an egg of comparable stage as a. f2: flat mounted of an early blastoderm, from an egg of comparable stage as f, DAPI stained (compound microscope). a–f, a1–f1, e2: Scale bar 200 μ m; a2–d2, e3: scale bar 100 μ m; d3, f2: scale bar 20 μ m.

at any one site showed typically only a 2–4 °C diurnal variation at all but the most superficial egg lay sites.

The mothers lay eggs in these chambers, and then coil around the clutch, dorsal side towards the eggs, remaining with the clutch

for more than 2 months, throughout embryogenesis and for the first several moults after hatching, until the young centipedes reach the adolescens I stage and are capable of feeding (Lewis, 1961).

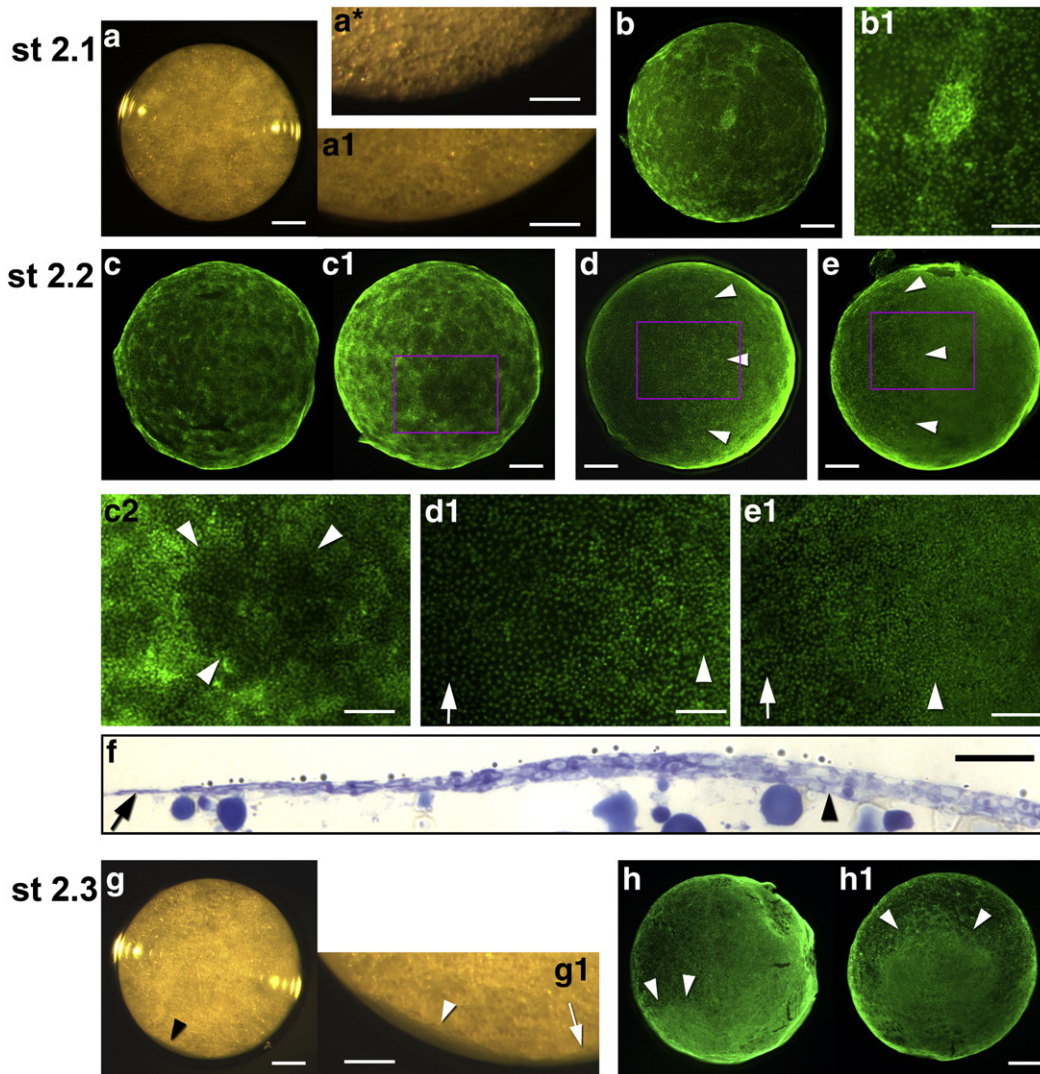


Fig. 2. Developmental stage 2, blastoderm, gastrulation and cephalic condensation: (a, a*, g) live eggs selected from a cohort of eggs that were photographed at regular intervals. (b–e, h) Fixed eggs at comparable stages. In this and subsequent figures, these have been dechorionated and nuclear stained with SYBR green to show the morphology. Pictures with letters followed by a number are different views or magnifications of the same embryo, e.g. b1 is an enlargement of b, etc. (a–b) Stage 2.1: A blastoderm covers the whole egg, forming a continuous lining at the edge of the yolk, visible in the living egg as a smooth edge to the yolk (a, enlarged in a1; compare this with the irregular edge visible in (a*)), which shows a similar view of the same egg 4 days earlier, before blastoderm formation. The distribution of nuclei is not completely uniform (b, b1). Remnants of the polygonal patterning of stage 1.4 are still visible in some parts of the egg. (c–f) Stage 2.2: the blastoderm becomes multilayered over somewhat more than one hemisphere of the egg (the future posterior, to the right in panels c, d and e, which show lateral views). Nuclei remain sparse within a small circular area near the middle of this multilayered region, which we identify as the blastopore (boxed in c1, enlarged and marked with arrowheads in c2. c1 is a posterior view orthogonal to c). As stage 2.2 progresses the multilayered region seems to extend from the blastopore towards the anterior of the egg (d, e). The transition between the single layered (arrow in d1, e1, f) and multilayered regions (arrowheads in d1, e1, f) is gradual and somewhat irregular around the circumference of the egg (f: toluidine stained section of an embryo at a similar stage to d–e). The transitional zone boxed in d and e is enlarged in d1, e1. (g, h) Stage 2.3: a thickening of the peripheral blastoderm is clearly visible through the chorion in one quadrant of the living egg (arrowheads in g, g1), revealing the condensation of the blastoderm in the cephalic area. The demarcation between this cephalic condensation and the sparser blastoderm surrounding it is now rather sharp (arrowheads in h (lateral view), and h1, ventral view, orthogonal to h). The multilayered blastoderm is now visible as a thin peripheral layer in the living embryo, posterior to the cephalic condensation (arrow in g1). Scale bars: 200 μm for whole egg views; 100 μm for enlarged panels (a1, b1, c2, d1, e1, g1); 20 μm for section in f.

The number of eggs per clutch is variable. Occasional females are found with only 2–3 eggs, others with up to 30 or more. For our 2010 collection, clutches averaged 13.3 eggs (mode 14, median 13; $n = 485$ clutches). The maximum recorded number was 34 eggs brooded by a single female.

Eggs of a single clutch are not precisely synchronous, but show a sequence of closely spaced developmental stages, suggesting that eggs are laid sequentially, and fertilised or activated as they are laid. For example, in 6 clutches of eggs fixed in the field during the mid stages of segmentation, the distribution of segment numbers covered a range of 9–12 segments, corresponding to a spread of age of about 30 h at 13 °C (2.5% of total development, see below). Interestingly, the range of developmental age within a clutch is not obviously correlated with the total number of eggs—the difference in stage

between the oldest and the youngest egg in a clutch of 29 eggs was similar to that for a clutch of 9 eggs. Observations of the timing of germ band flexure in cultured clutches show a similar distribution of ages (see Supplementary information).

The age range of embryos collected on a single date varies considerably, both among clutches at a single location, and even more markedly between sites which may be just metres apart on the beach, probably depending on the characteristics of each specific egg laying site, which will affect the depth at which eggs are laid, and thus probably the average temperature of the eggs' environment.

S. maritima eggs are spherical, averaging 1.1–1.2 mm in diameter (recorded extremes are 0.7 mm and 1.3 mm). They appear to be covered by a single envelope, the chorion. We have found no evidence for the presence of a distinct vitelline membrane. The chorion is 5–7 μm

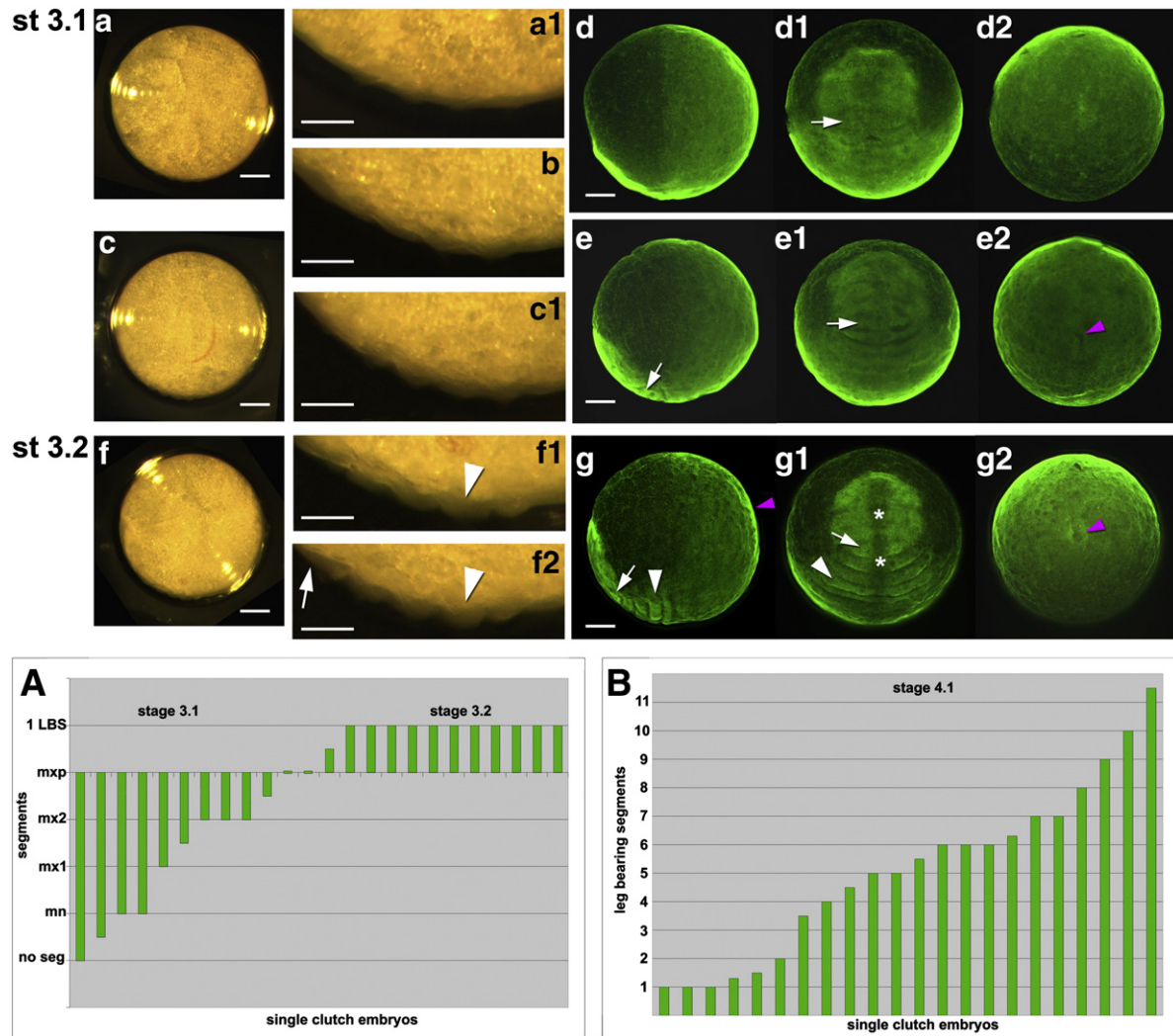


Fig. 3. Developmental stage 3, early phase of segmentation—appearance of anterior segments: (a, b, c, f) Live eggs. (d, e, g) Fixed eggs at comparable stages. Pictures with letters followed by a number are different views or magnification of the same embryo. (a–e) Stage 3.1: in live embryos (a–c), segments appear first as indistinct wrinkles in the cephalic condensation, becoming more pronounced as the stage progresses (sequence a1 to c1). In nuclear stained fixed embryos (d, e), the furrows demarcating the first five segments appear, starting with the mandibular (arrows in d1, e, e1). During stage 3 the “blastopore” transforms into a distinct invagination, the proctodeum (magenta arrowhead in e2). (f–g) Stage 3.2: the first five segments (mn, mx1, mx2, mxp, 1st LBS) are well defined by morphological ridges and can be recognised in living eggs (f), although not all of them can be seen, depending on the position of the egg (e.g. the view in f1 shows only 3 clear bumps, but in f2 the same egg, slightly turned, reveals 5 clear segments). Arrowheads: forcipular segment, arrows: mandibular segment, asterisks in g1 indicate forming midline tissues. Note that the mxp segment is distinctly wider than the following 1st LBS. Magenta arrowhead marks well formed proctodeum. (d, e, g: lateral view, ventral side on the bottom, d1, e1, g1: ventral view, d2, e2, g2, posterior view; second and third views orthogonal to the first). Scale bars: 200 μ m for whole egg views; 100 μ m for enlarged panels (a1, b, c1, f1, f2) (d–e, g: SYBR green nuclear staining). A–B: Diagrams showing the distribution of segment number in embryos from two single clutches at stage 3 and stage 4.1, comprising 24 and 22 embryos respectively, arranged in sequential order of developmental stage. At stage 4 (B) embryos within a clutch show a sequence of increasing number of leg-bearing segments (with a maximum of 2–3 embryos with the same number of LBS). On the contrary at stage 3 (A) the distribution of 13 embryos with 1 LBS would indicate a pause in the segmentation process that we identify with stage 3.2. mn: mandibular segment, mx1: first maxilla, mx2: second maxilla, mxp: maxilliped.

thick (after fixation), rather delicate when newly laid, but becoming darker, harder and quite brittle with age. It typically bears a number of small ring shaped brown marks, spaced in pairs about 60° apart around the egg circumference. The position of these marks bears no fixed relation to the axes of the future embryo, but may just mark the contact points between eggs within a clutch. No other marks or distinguishing features suggest or define axial asymmetries in the egg or future embryo.

The chorion is rather permeable to water—eggs will wrinkle and collapse if exposed to dry air for a few minutes or if immersed in full strength seawater, and most will burst if they are placed for some hours in distilled water. The chorion is also permeable to some other small molecules (e.g. formaldehyde), which allows them to be fixed without permeabilisation. It is not permeable to dyes such as DAPI or methylene blue. The composition of the chorion is not known; only extended periods (more than 10') in 50% bleach

will dissolve it (though this destroys the live or fixed embryos within much faster, in a few minutes). Attempts to digest the chorion with proteinases have been unsuccessful.

Culturing conditions and survival rates

In the field, geophilomorph centipede mothers protect their eggs for a prolonged period, but in the benign environment of the laboratory, a large proportion of *Strigamia* embryos will develop and hatch normally without this protection.

Over the past eight years we have used a number of different conditions to culture *Strigamia* eggs, generally either on filter paper moistened with saline, or immersed in a shallow layer of mineral oil within a humid chamber (see [Materials and methods](#)). The latter method has the advantage that the eggs are largely protected from desiccation, and the developmental stage of older eggs can be quickly

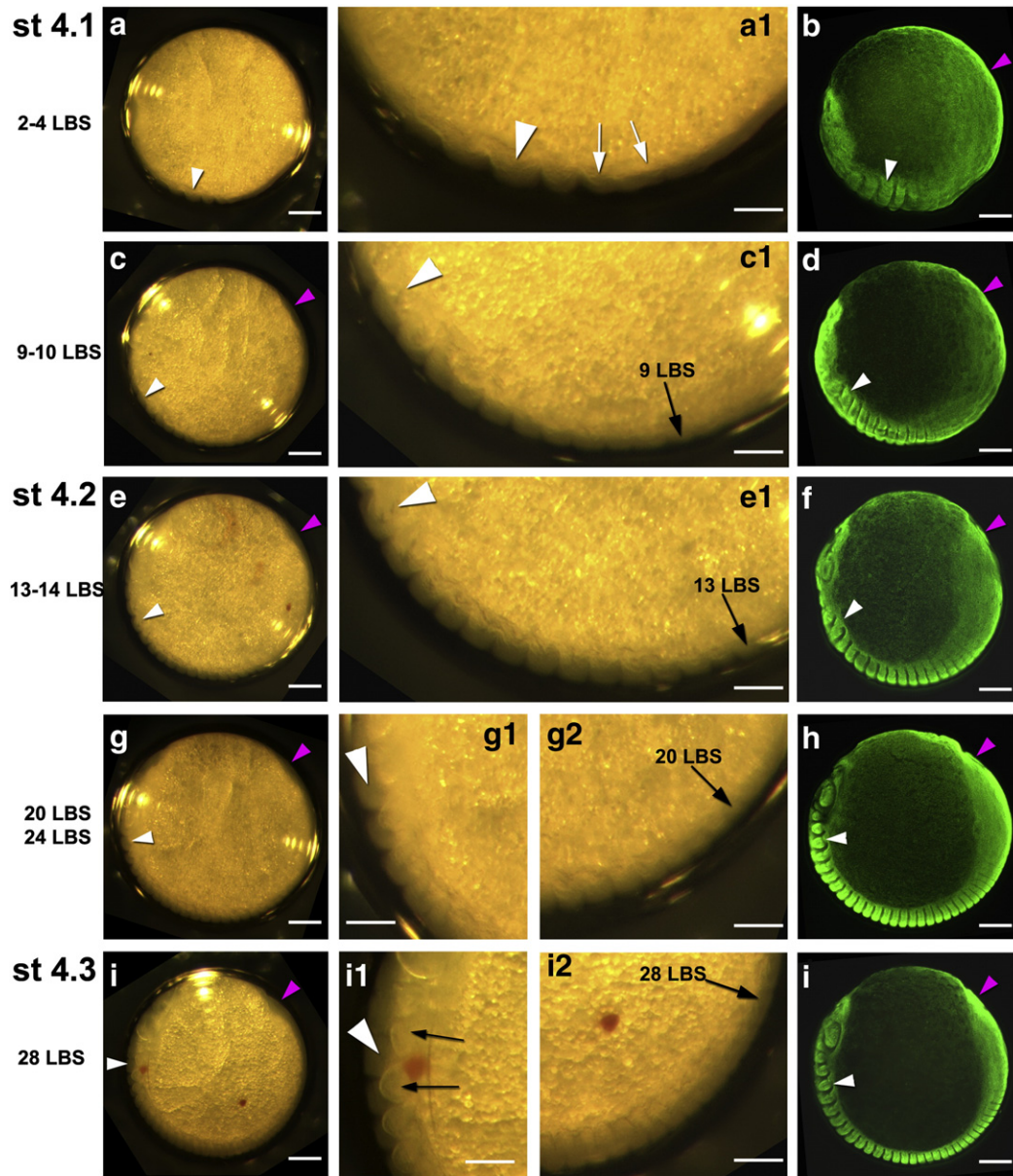


Fig. 4. Developmental stage 4, main phase of trunk segment addition: (a, c, e, g, i) Live eggs. (b, d, f, h, j) Fixed eggs at comparable stages. Eggs have been oriented to match comparable frames of the time lapse movies, so that their positions should reflect the relative movement of the different parts of the germ band in relation to the underlying yolk. Pictures with letters followed by a number are magnifications of the same embryo. In all panels, a white arrowhead marks the fornicular segment and a magenta arrowhead marks the position of the proctodeum. Panels 4a and 4i show the same specimen as panel 3f, 1 and 4 days later in development. (a–d) Stage 4.1: behind the 1st LBS, trunk segments appear sequentially (arrows in a1). The anterior part of the forming germ band extends anteriorly, (compare beginning and mid stage 4.1 (b and d)). (e–h) Stage 4.2: the anterior margin of the germ band has stopped extending forward, while the proctodeum continues to extend backwards; the extent of the MLB is reduced to a more defined posterior disc. The segments of the head have compacted and rearranged substantially during stages 4.1 and 4.2 (compare panels b and h). (i–j) Stage 4.3: the proctodeum has stopped extending backwards. The hemitergite primordia of the most anterior trunk segments are visible as distinct lateral bumps, even through the chorion (arrows in (i1)). Scale bars: 200 μm , except pictures at high magnification (a1, c1, e1, g1, g2, i1, i2: scale bar 100 μm) (b, d, f, h, j: SYBR green nuclear staining).

scored without handling the individual eggs, but it is not so convenient if the eggs are to be fixed or injected.

The strength of the chorion allows the eggs to tolerate a range of osmotic pressures. In the laboratory, eggs will develop normally on anything from 0.5 \times to at least 1.5 \times concentrations of PBS or insect saline (approximately 75 mM to 225 mM salt). At the lower concentrations the increased turgor pressure of the eggs makes them more liable to burst when handled.

For the studies reported here, we have normally kept eggs at 13 $^{\circ}\text{C}$, though eggs will develop well at temperatures between 10 and 20 $^{\circ}\text{C}$, with comparable survival rates. In a sample of 672 field collected eggs maintained in mineral oil at 13 $^{\circ}\text{C}$ without disturbance, 90% completed the main phase of segmentation, and 67% reached

the adolescens I postembryonic stage (after 14 weeks). The survival rate of eggs regularly checked under the microscope is lower (see Supplementary materials). Those eggs that die generally succumb to fungal infections, but whether this is a cause or consequence of death we do not know.

Embryos developing at 25 $^{\circ}\text{C}$ show many abnormalities. At 8 $^{\circ}\text{C}$ eggs develop apparently normally, but most fail to hatch. Eggs will survive at 4 $^{\circ}\text{C}$ for up to 3 months, developing very slowly, and will frequently recover when returned to 13 $^{\circ}\text{C}$. However, the proportion of undeveloped and abnormal embryos increases steadily as the time at 4 $^{\circ}\text{C}$ extends, for example rising above 80% undeveloped after 11 weeks (see Supplementary Fig. S1). Importantly, when pre-segmentation stage embryos are kept for a period at 4 $^{\circ}\text{C}$, this seems

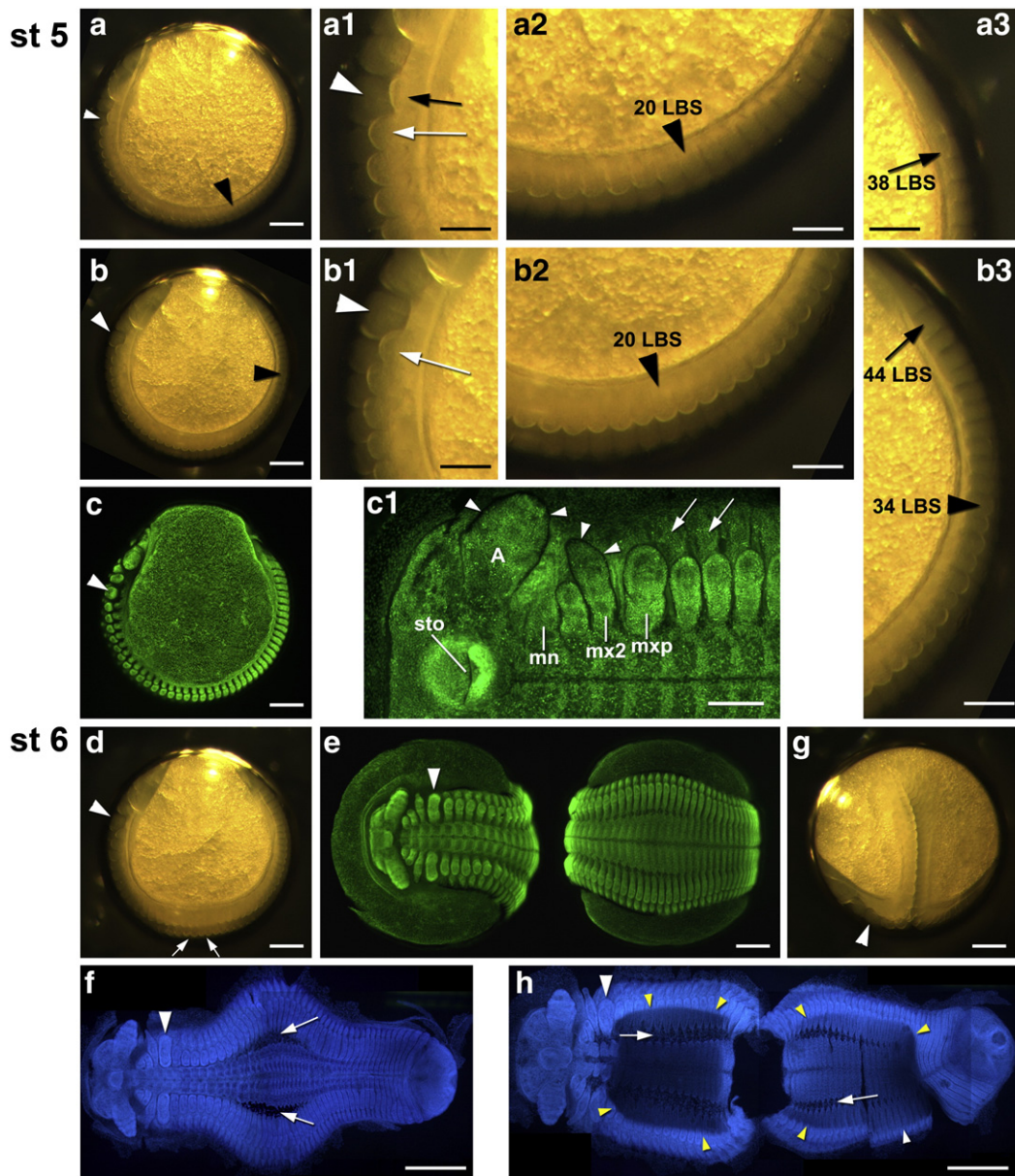


Fig. 5. Developmental stages 5 and 6, pre-flexure segmentation and dorso-ventral flexure: (a, b, d, g) Live eggs; (c, e, f, g, h) Fixed eggs at comparable stages, dechorionated and nuclear stained (c, e: SYBR green; f, h: DAPI), and flat mounted (c1, f, h) to show the morphology. Arrowhead marks forcipular segment in all panels. Panels 5b, 5d and 5g show the same specimen as panels 3f, 8, 9 and 10 days later in development. Stage 5: (a, b) early and late stage 5. At the beginning of this stage, the bulge marking the hemitergite primordium of the forcipular segment (black arrow in a1) is smaller than those of the 1st LBS (white arrow) and following segments. It becomes almost invisible by the end of the stage (b1). At the beginning of the stage, hemitergite primordia are visible as distinct bulges up to about the 20th LBS (black arrowhead in a, a2), which lies diametrically opposite the anterior end of the germ band. In later stage 5, hemitergite primordia appear progressively closer to the posterior end of the segmented region (black arrowhead in b, b3). (c) Fixed embryo of late stage 5. (c1) Flat mount of the same embryo showing arrangement of the head segments (A—antennal bud; mn—mandible; mx2—second maxilla; mxp—maxilliped; sto: stomodeum; arrows: hemitergite primordia of the 1st and 2nd LBS). This embryo has been processed for *in situ* hybridisation. Characteristically at this stage, a dark non-specific stain (arrowheads) outlines the limb buds of the head, probably reflecting the first secretion of embryonic cuticular matrix. Stage 6, dorso-ventral flexure: The first signs of flexure are a slight flattening of the germ band away from the chorion (arrows in d) and the lateral spreading of the midpart of the germ band (e). The whole germ band then folds and sinks into the yolk (f–h; the germ band in h was folded similarly to that in g, and has been broken at the fold to flatten it). As the germ band spreads a thin epithelium is interposed between the medial and lateral parts of the germ band (arrows in g and h). Scale bars: 200 μm , except pictures at high magnification (a1, a2, a3, b1, b2, b3, c1: scale bar 100 μm). Note that the juxtaposition of the anterior and posterior parts of the germ band within the yolk presents a partial barrier to staining of the ventral regions. These appear only weakly stained in h (area marked by yellow arrowheads).

to affect their initial rate of development after return to 13 °C. The blastoderm stage is considerably extended. Once segmentation has started, though (from stage 4 on, see below), their timing aligns with that of all other embryos.

A staging series for embryonic development

To establish a staging series for development, and to define the duration of each stage, our primary reference has been a series of clutches collected from the field, and reared throughout embryogenesis to hatching

and beyond. For some clutches, eggs were photographed regularly throughout development; for others, eggs were sampled and fixed at known intervals (see [Materials and methods](#)).

We have in addition taken videos of living embryos for periods of up to 4 days, particularly during stages of segment formation and sinking, when morphological changes are clearly apparent. Unfortunately, the embryo tends to rotate within the chorion during development. This, together with the extended total period of development, makes time lapse observation a somewhat problematic tool to follow

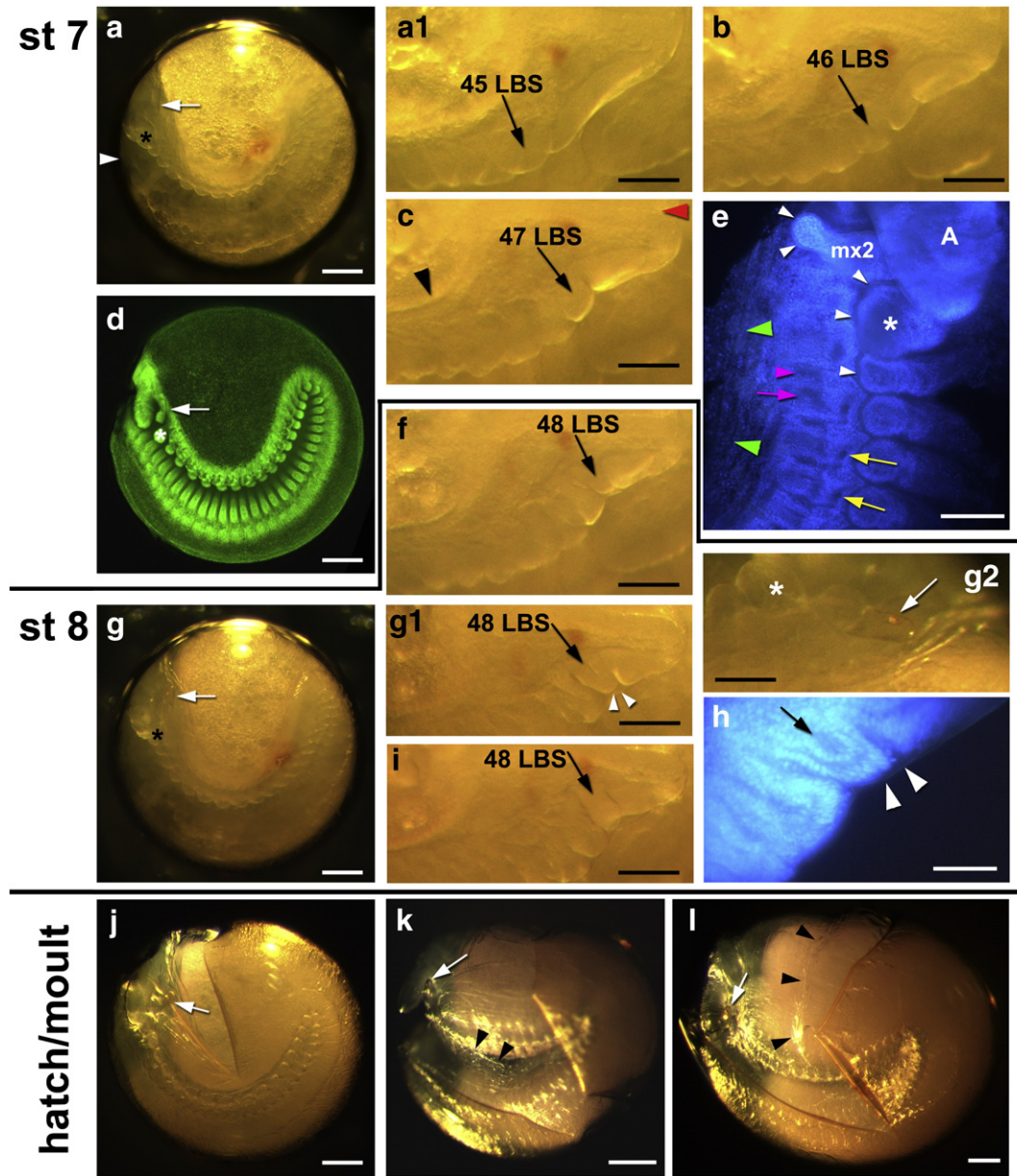


Fig. 6. Developmental stages 7–8 and hatch/1st moult: (a, b, c, f, g, i, l) Single live egg photographed at regular intervals (a–b–c–f–g: 1 day, g–i: 2 days, i–l: 8 days). (a1, b, c, f, g1, i: dorsal view of the left half of the posterior of the embryo, viewed through the chorion, from a point of view as indicated by the arrowhead in a; anterior to the left); j, k live eggs selected to show additional key phases of hatching/moulting. Pictures with letters followed by a number are magnifications of the same embryo at the same stage. (d, e, h) Fixed eggs at stages comparable to a, b, f, respectively, dechorionated and nuclear stained (d: SYBR green; e, h: DAPI), and flat mounted (e, h) to show the morphology. Alphabet order reflects developmental sequence. (a–e) Stage 7 embryos: dorso-ventral flexure is complete. The second maxilla now lies dorsal to the antenna (arrow in a and d). During stage 7, two additional segments appear at the posterior of the germ band (46 and 47 in this specimen) (a1–c); in panel 6c are indicated the developing Malpighian tubule (black arrowhead) and the proctodeum (red arrowhead). (e) By about 2 days after dorsal flexure, a cuticle (white arrowheads) is well formed around the anterior limb buds (A—antenna; mx2—second maxilla; asterisk—forcipule). Presumptive tracheal pits have formed (yellow arrows). The hemitergite primordia are differentiating into pretergite (pink arrowhead) and metatergite (pink arrow), and are extending latero-dorsally in the early phase of dorsal-closure (green arrowheads). (f–h) Early stage 8 embryos: an egg tooth has formed on top of the second maxilla (arrow in g and g2); the two last leg-bearing segments are formed during stage 8. The first of these is visible in early stage 8 (arrows in f–h), beneath a detached embryonic cuticle that shows no imprint of this limb bud (arrowheads in g1 and h). h shows a single optical section of a flat mounted embryo, revealing the mesoderm already distinct within this limb bud. By mid-late stage 8 it is no longer possible to see clearly through the chorion. (j) Recently hatched egg. The chorion has cracked over the egg tooth (arrow), and is gaping somewhat open. (k) An egg 1–2 days after hatching. Movements of the embryo within the hatched egg have revealed a loosened cuticle that appears to bridge the juxtaposed anterior and posterior parts of the embryo (arrowheads). (l) An egg 2–3 days after hatching. The embryo, now larva, has begun ecdysis, breaking the embryonic cuticle dorsally just posterior to the head (arrowheads mark the anterior margin of the dorsal exuvia). Both larva and exuvia remain within the broken chorion. Asterisk: forcipular segment, white arrow: second maxilla. (a, d, g, j, k, l: scale bar 200 μ m; a1, b, c, e, f, g1, g2, i: scale bar 100 μ m; h: scale bar 50 μ m).

Strigamia development (see [Materials and methods](#)). Time lapse has been very helpful, though, in understanding the relative movements of the anterior and posterior parts of the forming germ band.

We have also examined the diversity of stages present in single fixed clutches. Each clutch presents a series of closely spaced stages spanning 2–3% of development (see above). This has been particularly useful to

establish the sequence of early stages, when little is visible in live embryos (e.g. diagrams A and B in [Fig. 3](#)).

The stages defined below correspond broadly to those defined by [Chipman et al. \(2004b\)](#) and partly subdivided by [Chipman and Stollewerk \(2006\)](#). However, we now realise that the period before the first appearance of segments is much longer than previously

thought, and that the visible changes to the yolk are a poor guide to developmental stage during this early period. We have redefined Chipman stages 1–3 to reflect this. We have also slightly modified the definitions of segmentation stages 4–6 to reflect distinct phases of the segmentation process, and have subdivided Chipman's final stage 7 into stages 7 and 8 (see [Discussion](#)). Of course, development is a continuous process, and in some cases, it is not possible to define a precise point at which one stage transforms into another.

For stages 1–3 below, a brief description of what is visible in whole live or fixed eggs (*in italics*) is followed by a summary of the morphology visible in stained embryos after dechorionation. From stage 4 onwards, visible morphology is sufficient to define each stage, so we do not make this distinction in the stage descriptions. For each stage, further comments note points additional to the stage description—e.g. ambiguities, uncertainties and further inferences.

All durations given below are for culture at 13 °C, in lab conditions.

A table summarising the staging characters is included as Supplementary material (Table S2).

Stage 1: Cleavage and peripheral migration

Duration : 22 days

Cells divide at the centre of the egg and then migrate to the egg surface, following the spaces between yolk pyramids. No cellular morphology is visible externally in living eggs until stage 1.4 (Fig. 1).

Stage 1.1: (Figs. 1a–b) Early cleavage

Duration: approx 9 days

External appearance: Eggs white or cream; yolk initially uniform, almost transparent appearance. At the very earliest stages (Fig. 1a and before) the chorion is weak and elastic, and eggs burst particularly easily when handled.

The zygote nucleus lies within a region of actin-rich cytoplasm near the centre of the egg. It divides to generate first a few large blastomeres (Figs. 1b1–2), and then a population of some tens of smaller cells. The yolk becomes partitioned radially into wedges (yolk pyramids) (Sograff, 1882), that are clearly visible only in fixed eggs (Figs. 1b1–2). Actin filaments extend from the central cytoplasm along the inter-pyramidal lines (Fig. 1b2).

Comment: It is not clear whether the yolk pyramids are initially continuous with the first cleavage blastomeres, i.e. whether the first cleavages of the egg are total.

Stage 1.2: (Fig. 1c) Late cleavage

Approx duration: 9 days

External appearance: Eggs yellowish to yellow (Fig. 1c); occasionally the irregular shapes of yolk pyramids are visible on the surface as fine lines defining partial polygonal patterns, particularly in fixed eggs.

Continuing division gives rise to a population of from several hundreds to several thousands of cells, still forming a compact cluster near the centre of the egg. These cells are smaller than in stage 1.1 (e.g. approx 15–20 µm diameter in Figs. 1c1–2). By the end of stage 1.2, there are a few thousand cells (picture not shown).

Comment: Distinct cells are clearly visible in live dissected eggs (Supplementary Fig. S3), and in fixed sectioned eggs (showing a cellularization level similar to the one indicated in Fig. 1d3), but we cannot rule out the existence of cytoplasmic bridges between cells.

The darkening of the eggs is partly due to the yolk acquiring a yellow colour, but mostly to the darkening (tanning?) of the chorion, which in the following stages will assume a brownish colour. Note that the extent of darkening appears to be variable between clutches, and eggs cultured in the lab occasionally fail to darken at all.

In a small proportion of the eggs examined (4 of 33), the initial mass of cells was clearly off centre, but we do not know whether this asymmetry correlates with subsequent egg axes.

Stage 1.3: (Fig. 1d) Cell migration

Approx duration: 3 days

External appearance: indistinguishable from previous stage (Fig. 1d).

Cells are migrating from the centre towards the periphery of the egg, following the boundaries between yolk pyramids, but they have not yet reached the egg surface (Figs. 1d1–3). Cell size is now similar to that of blastoderm cells, with nuclei about 7 µm in diameter.

Comment: There appears to be no obvious asymmetry to the migration, but the paths taken appear somewhat random, conditioned by the irregularity of the yolk pyramids.

Stage 1.4: (Fig. 1e) “Soccer ball” stage

Approx duration: 1 day

External appearance: Cells arriving at the egg surface are sometimes visible through the chorion as broad opaque whitish bands forming an irregular polygonal pattern at the surface of the yolk (Fig. 1e), not to be confused with the sharp boundaries of the yolk pyramids, which are generally only clear in fixed embryos. This visible pattern is transient and not seen in all eggs at this stage.

Thousands of cells reach the egg surface almost simultaneously, marking the outlines of the irregular yolk pyramids to generate bands of cells that appear as a striking “soccer ball” pattern visible after nuclear staining. Lagging cells initially remain in the inter-pyramidal spaces (Fig. 1e1). As the last cells reach the surface, others begin to spread to generate the blastoderm (Fig. 1e2, bottom of the egg; Fig. 1f). Cells continue to divide at the egg surface (Fig. 1f2).

Comment: Sections of blastoderm and later stages (data not shown) indicate that some cells remain interspersed in the yolk. We interpret these as yolk cells/vitelophages. We have no data showing whether these are left over from the process of cell migration to the surface, and/or whether they are cells that have delaminated from the blastoderm and migrated back into the yolk.

Stage 2: Blastoderm, gastrulation and cephalic condensation

Approx duration: 5 days

A layer of cells covers the whole egg surface, initially forming a near uniform monolayer, later becoming multilayered over more than half of the egg. The anterior part of the multilayered blastoderm converges anteroventrally to form the cephalic condensation.

Stages 2.1–2.2

Approx duration: 4 days

External appearance: Stages 2.1 and 2.2 are not externally distinguishable (Fig. 2a), and often appear very similar to stages 1.2 and 1.3. The formed blastoderm of stage 2, though, forms a faint opaque covering over the yolk and defines a continuous smooth outline when the yolk is viewed at the margin of the egg (see for comparison the same egg observed at stage 1 (Fig. 2a) and stage 2 (Fig. 2a1)).*

Stage 2.1: (Figs. 1f, 2b) Early blastoderm

Cells cover the entire surface of the egg, forming a mostly monolayered blastoderm (Figs. 1f1–2; Figs. 2a–b) comprising 20–30,000 cells (estimated for the eggs in Figs. 1f1, and 2b). At the beginning of this stage, the polygonal outlines of the interpyramidal spaces may still be visible (Figs. 1f1, 2b). A single localised cluster of tightly packed cells is transiently visible in one region of the egg (Figs. 2b, b1). This is no longer visible at stage 2.2.

Comment: Continuity in expression of certain marker genes, like *decapentaplegic*, suggests that the tightly packed cluster of cells visible at this early stage comes to occupy the region where the blastopore will form (Brena, unpublished data).

Stage 2.2: (Figs. 2c–f) Multilayered blastoderm/gastrulation

Part of the blastoderm is multilayered. This multilayered area is centred on a restricted circular region 200–300 µm in diameter that

remains covered by only a single layer of cells (Figs. 2c1, c2). We refer to this region as the blastopore. As stage 2.2 progresses, the multilayered part of the blastoderm (MLB) extends from the blastopore, eventually covering about two thirds of the egg surface. The edge of the MLB is irregular (Figs. 2d, e), grading rather smoothly at its edges into a single layer of more attenuated cells (Fig. 2f).

Comment: We have no indication of how gastrulation takes place, i.e. whether it occurs by invagination of sheets of cells, or by the delamination of individual cells. None of this is visible in living embryos.

Stage 2.3: (Figs. 2g–h) Cephalic condensation

Approx duration: 1 day

External appearance: A marked thickening of the cytoplasm is visible in lateral view as a clear layer between the chorion and the yolk surface in one quadrant of the egg (Fig. 2g1). This is the first morphological stage that can be scored with certainty, and relative ease, in all eggs. This thickening represents the forming cephalic area (Fig. 2h).

The extent of the MLB is somewhat reduced from its maximal extent in stage 2.2. Cells in its anterior part have condensed/converged to generate a thicker cephalic region, that is distinctly bounded and flanked on 3 sides by single layered blastoderm. The posterior half of the egg is still covered by a largely uniform MLB.

Comment: Cephalic condensation is probably associated with the forward extension of the ventral part of the MLB.

Stage 3: Early phase of segmentation—appearance of anterior segments

Approx duration: 2 days

The anterior segments become visible in quick succession within the cephalic condensation.

Stage 3.1: (Figs. 3a–e) First appearance of segmental furrows

Approx duration: 1 day

External appearance: Small bumps or wrinkles (up to 5) appear in the thickened cephalic area, representing the first morphological appearance of segments. It is difficult at this stage to identify specific segments through the chorion.

Variations in nuclear staining (probably reflecting differences in the distribution of meso/endoderm and ectoderm) define a characteristic pattern of forming segments at the interface between the cephalic region and the rest of the MLB (Figs. 3d–e). The mandibular segment (mn) is the first to be clearly defined by two furrows. Furrows defining the posterior of the following 4 segments (1st maxilla (mx1), 2nd maxilla (mx2), maxilliped/forcipular (mxp), and 1st leg-bearing segment) (1st LBS) appear in succession, anterior to posterior, one after the other (Figs. 3d–e). At the beginning of this stage, the blastopore is reduced to a small area corresponding to the proctodeum proper. It shifts towards the posterior of the MLB as development progresses (Figs. 3d–e).

Comment: Although nuclear staining suggests that the five segments from the mandibular to the 1st LBS arise sequentially, the wrinkles and bumps that define them rise almost simultaneously, making it difficult to identify specific segments from external appearance (see sequence Figs. 3a1, b, c1). Segments anterior to the mandibular are not delimited by full transverse furrows.

Stage 3.2: (Figs. 3f–g) Clear demarcation of five anterior segments

Approx duration: 1 day

External appearance: Five anterior segments are clearly demarcated by furrows (the mandibular to 1st LBS), though it remains difficult to see them all from any single angle of view (see for example the same embryo from different points of view in Figs. 3f1–f2). The bulge of the 1st LBS is distinctly smaller than that of the mxp, allowing these segments to be defined unambiguously, even if only 3 “bumps” are visible (see beginning of Timelapse 1).

By this stage, the contours of the five anterior segments are well elevated on the egg surface. The extension of the cephalic region is reduced, and the lateral parts of these segments are visibly distinct from the midline tissues (asterisks in Fig. 3g1). The remaining MLB posterior to the cephalic region covers about half of the egg, and can now be described as a posterior disc. The proctodeum appears as a narrow invagination with an elevated thickened rim, lying close to the middle of this posterior disc.

Comment: There appears to be a pause in segment addition at this 5-segment stage. Eggs observed daily retained this morphology on successive days, and embryos with this appearance are relatively frequent in collections of eggs fixed at random stages. Single clutches fixed around this stage contain a relatively large number of eggs with precisely these five segments visible, while the slightly younger and older eggs in the same clutches show sequential numbers of segments (Fig. 3 diagrams A and B).

Stage 4: Main phase of trunk segment addition, from 2 to ≈ 39 LBS

Duration: 5 days

Leg-bearing segments from 2 to ≈ 38 are added sequentially. The germ band extends through the reorganisation of the MLB/posterior disc, the width of which shrinks progressively.

(Note: During segment addition, the number of leg-bearing segments can conveniently be used to describe the stage of the embryo, but given the variability in final adult segment number, it should be born in mind that embryos with the same segment number may in fact be at slightly different developmental stages. This is particularly true for embryos near the end of segment addition).

Stage 4.1: (Figs. 4a–d) [Supplementary material: Timelapse movie 1 (TL1), beginning; TL2 starts at mid stage 4.1]

Duration: 1.5 day

2 to ≈ 13 LBS defined by visible furrows.

As these segments appear, both the anterior margin of the germ band and the proctodeum extend around the egg, in opposite directions. The proctodeum approaches more closely the posterior edge of the posterior disc.

Stage 4.2: (Figs. 4e–h) [Supplementary material: TL1 around 17/08/2009 12:10:51, TL2 at: 05/09/2009 00:00:01, TL3 from beginning]

Duration: 1.5 day

≈ 14 to ≈ 27 LBS defined by visible furrows.

At about the 14 LBS stage the anterior margin of the cephalic region ceases to extend forward over the yolk, while the posterior part of the germ band, and in particular the bulge associated with the proctodeum, continues to extend backwards. Simultaneously, the more anterior (older) segments condense, reducing both the length and the width of the cephalic region.

Stage 4.3: (Figs. 4i–j) [Supplementary material: TL2 around 5/9/09 19:01:11]

Duration: 1 day

≈ 28 to ≈ 39 LBS defined by visible furrows.

The proctodeum and posterior margin of the germ band have ceased to extend: the germ band has reached its definitive length.

At the beginning of this stage, “lateral bumps” become clearly visible on the first trunk segments (mxp to 2nd–3rd LBS; Fig. 4i1, arrows). These represent the distinction between the limb primordia and the forming hemitergites; the hemitergite primordium of the mxp is smaller than those of the leg-bearing segments. The hemitergite primordia are already forming at mid stage 4.2, but are not distinct enough to be clearly detected through the chorion (Fig. 4g1; see also flat mounted embryos in Fig. 7).

Comment: Throughout stage 4, segments are added at a uniform rate, about one segment every 3.2 h at 13 °C (see below).

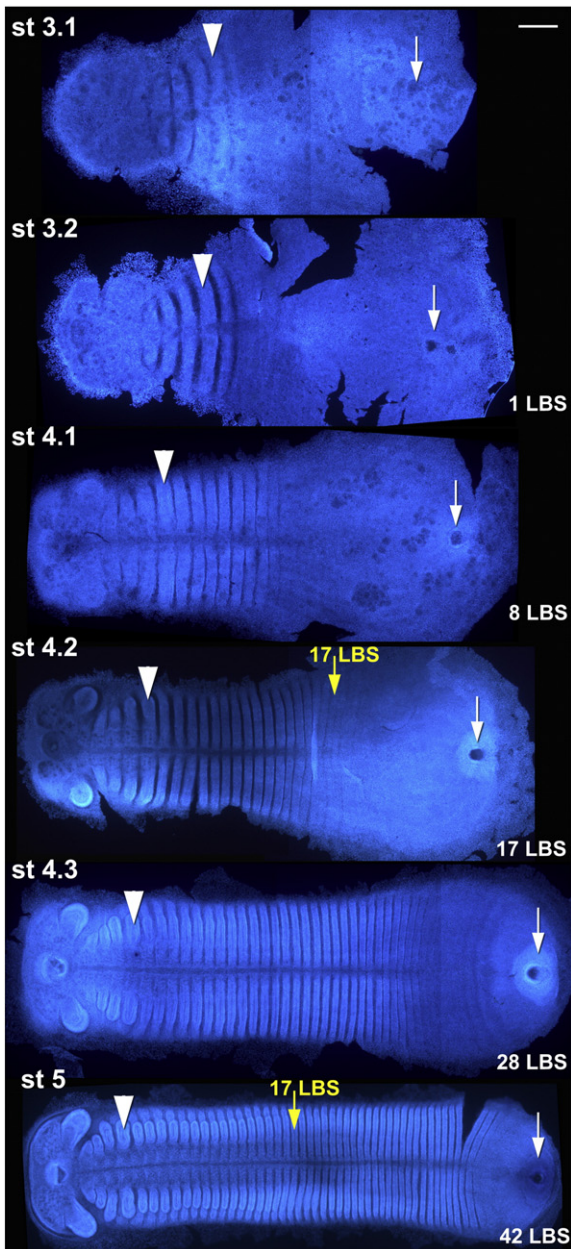


Fig. 7. Relative proportions of the germ band through segmentation: Selected embryos, nuclear stained (DAPI) to show the morphology, dissected and flat mounted to show the relative extension and compaction of different parts of the germ band. The photos are all at the same scale, and have been aligned in the A/P axis to match the position of the embryo seen in time lapse movies. In all panels, an arrowhead marks the forcipular segment, and a white arrow the proctodeum, which is just appearing at stage 3.1 (top panel). A yellow arrow marks the 17th LBS, just appearing at stage 4.2. Lateral parts of the multilayered blastoderm have been trimmed in the photos of stages 3.1–4.2. (Note—in the embryo at stage 4.3, the pattern of dark crescents anterior to the proctodeum results from an in situ hybridisation stain. It does not reflect morphology.). Scale bar 100 μ m.

Stage 5: Late, slow, phase of pre-flexure segmentation

Approx duration: 3 days

\approx 40–45 leg-bearing segments defined by visible furrows

(Figs. 5a–d)[Supplementary material: TL2 around 6/9/09 00:01:10, with \approx 38 LBS]

Segment addition slows down as the last few (\sim 4) pre-sinking segments are added. The posterior disc is no longer wider than the germ band. The segmentation front approaches the proctodeum. The mx2 appendage becomes longer than the mxp and develops a

pointed tip. Subdivision of the antennae into antennomeres starts to be apparent towards the end of this stage.

At the start of stage 5, forming hemitergites are well defined by lateral bumps up to about the 20th LBS (Fig. 5a). By the end of stage 5 they are visible on most segments (all but about the last 6 LBS) (Fig. 5b, beginning of TL4).

During this stage the germ band continues to narrow, and to become more three dimensional. Deposition of the embryonic cuticle begins, starting with the more anterior limb buds (arrowheads in Fig. 5c1).

Comment: From this stage onwards, in situ hybridization probes are often trapped non-specifically by the forming cuticular matrix.

Stage 6: Spreading and dorso-ventral flexure

Duration: 2 days

The germ band stretches medio-laterally and then flexes into the yolk near its midpoint, eventually bringing the ventral surfaces of the anterior and posterior halves of the germ band into apposition.

Stage 6.1: Germ band spreading, flexure and sinking to 25% egg diameter (Figs. 5d–f) [Supplementary material: spreading: TL4 around 23/8/09 16:55, flexure: TL4 around 24/8/09 05:35, beginning of TL5]

The first signs of flexure are the lateral spreading of the germ band at the midpoint of the germ band (Fig. 5e), and a slight flattening of the germ band away from the chorion at this midpoint (Fig. 5d). Further spreading happens through the interposition of monolayered epithelium between the medial tissues (neuroectoderm and ventral ectoderm) and the dorso-lateral tissues of the germ band, with the associated limb buds (Fig. 5f). The initial flattening of the germ band becomes a concave dip, and then the germ band flexes sharply into the yolk, starting to bring the ventral surfaces of the anterior and posterior halves of the germ band into apposition.

Stage 6.2: Flexure from 25% to 75% egg diameter

(Fig. 5g) [see Supplementary material: TL4 from 24/08/2009 07:35:15 to 24/08/2009 09:55:15, and TL5 approximately from 14/08/2007 19:51:15 to 14/08/2007 23:41:15]

This is the fastest phase of the movement. During this stage, in lateral view, the margins of the two juxtaposed parts of the embryo lie parallel (see TL4). At the end of this stage the anterior and posterior parts of the segmented germ band are facing one another throughout most of their length, and the folded germ band is just beginning to flex into a J shape.

Stage 6.3: Flexure above 75% egg diameter

(Fig. 5h)

Most of the germ band is ventrally juxtaposed, and the folded germ band is flexed into a J shape. The anterior and posterior extremes of the embryo are still on the surface (Fig. 5h), gradually approaching one another as the head and tail fold together.

Comment: Sinking begins and ends slowly but is rapid in its middle stages. This dramatic morphogenetic movement allows for precise staging of living eggs as they pass through stage 6.2. By the time sinking is complete, stains such as Dapi are partially prevented from reaching the ventral parts of the germ band that are tightly juxtaposed (see Fig. 5h).

Post-sinking stages

During stages 7 and 8, it is difficult to observe details of segment morphogenesis through the chorion, partly because of the tight juxtaposition of the folded germ band, but also because of the formation of the first embryonic cuticle and its apolysis. This cuticle makes staining difficult on dechorionated whole late stage 7 embryos, and virtually impossible in stage 8 embryos, after apolysis. Detailed description of

these later stages will require sectioning and/or dissection of the embryo, and is beyond the scope of this paper. However, we describe two provisional stages within this later part of development, demarcated by the first embryonic apolysis.

Stage 7: Post-flexure, pre-apolysis development

(Figs. 6a–e) (TL4 around 24/8/09 15:35, TL5 around 15/8/07 7:21)
Approx duration: 4 days

Dorso-ventral flexure has been completed. The germ band is tightly folded in two, with the head facing the proctodeum, and the juxtaposed anterior and posterior halves in close contact. The antennae have moved ventral to mx2. Segmentation is resumed with the addition of 2 further segments (Figs. 6a–e) as the posterior of the embryo becomes more elongated. In association with this, the hindgut, which now lies parallel to the egg surface, elongates. The midgut, enclosing the yolk, narrows and Malpighian tubules extend forwards from the midgut/hindgut junction, flanking the midgut (black arrowhead in Fig. 6c).

The mx2 extends faster than the other limb buds, and now protrudes markedly; presumptive tracheal pits are visible in the anterior segments, and the hemitergites of these segments start to extend dorsally (Fig. 6e). Pretergite and metatergite can already be distinguished (Fig. 6e). Despite the developmental delay of the more posterior segments, dorsal closure starts earlier in the posterior half of the embryo, which encloses less yolk than the anterior.

The forming cuticle tends to bridge between the anterior and posterior halves of the embryo, just internally to the limb buds, as is clear at the 1st moult after hatching (arrowheads in Fig. 6k). This may explain why in folded embryos (from mid stage 6 onwards), probes and stains have limited access to the ventral areas (seen as darker in Fig. 5h, because nuclei in this region are not efficiently stained by DAPI)

Stage 8: Embryonic apolysis, egg tooth darkening, formation of the last 2 leg-bearing segments

(Figs. 6f–i)
Approx duration: 6 days

The beginning of this stage is defined by the tanning of the cuticle at the tip of the 2nd maxilla, particularly in one spot, the egg tooth (Figs. 6g, g2). This is associated with the beginning of apolysis of the embryonic cuticle, wrinkles of which are clearly visible posterior to the head (Fig. 6g). This becomes clearer later, when cuticle is visibly detached in several areas (e.g. the tip of the antenna).

Eggs at this stage become pink, due to pigmentation in the yolk, typically getting darker with age. The timing of appearance of this pigment is not a fully reliable character. Some clutches never develop strong pigmentation under culture conditions (e.g. the one shown in Fig. 6j).

The embryo at this stage shows frequent peristaltic movement of the gut, engulfing the whole yolk (this is particularly clear in the anterior enlarged part of the trunk).

The furrow between the two last leg-bearing segments appears at the beginning of stage 8 (Fig. 6f). These two segments lie under a single cuticle bulge at this stage (arrowheads in Figs. 6g1 and h), indicating that the furrow between them forms after the apolysis. The furrow defining the posterior of the last leg-bearing segment is defined later, and can only be seen after hatching, by artificially removing the chorion and exuvia.

Hatching and first embryonic moult (Figs. 6j–l)

Hatching is defined by the cracking of the chorion (Fig. 6j), but the embryo/larva remains inside the cracked chorion for a considerable time thereafter. About a day after hatching the embryonic cuticle splits across a dorsal line posterior to the head (arrowheads in 6l), but this ecdysis is incomplete.

This and subsequent exuviae remain attached to the posterior extreme of the larva until at least the peripatoid stage, at least in our culture conditions. These early post-embryonic stages will be described in more detail separately (Brena, in preparation).

Modification of the germ band proportions through time

During stages 3 to 5 of *Strigamia* development, the original multi-layered part of the blastoderm (MLB) condenses to form the germ band, as segments appear sequentially from anterior to posterior.

Once the first segmental furrows have formed, and the head is morphologically defined, it is possible to dissect the forming germ band from the yolk, and to mount it flat on a slide. In Fig. 7, such flat mounted embryos have been aligned in the A/P axis such that the relative positions of the head and proctodeum reflect the movements of the germ band over the yolk, as observed in the timelapse videos.

At the earliest of these stages, the MLB still covers almost one whole hemisphere of the egg, with only the anterior part of the germ band clearly protruding and sharply demarcated from the surrounding attenuated epithelium (Figs. 3d, g). It is impossible to flatten this structure into two dimensions without some distortion, particularly in the medio-lateral axis (hence the splits in the embryos at stages 3.1 and 3.2 in Fig. 7). However, comparison of flat mounted embryos with live embryos and time lapse videos shows that there is little distortion in the A–P axis (data not shown). As the MLB condenses into a smaller posterior disc, this distortion becomes less pronounced.

Fig. 7 illustrates important aspects of the dynamics of germ band formation. First, the overall extension in length is modest—the distance from the anterior of the head to the proctodeum increases only about 40% from stage 3.1 to stage 4.3, by which time the germ band has reached its final length. However, the relative proportions of different regions of the germ band change significantly. The head, (i.e. that part of the germ band anterior to the forcipular segment), initially spans 40% of this total length, but condenses in absolute and relative terms until by stage 5 it occupies less than 20%. The most anterior leg-bearing segments show a similar condensation, such that the relative position of any given segment moves forward in the germ band as development proceeds (e.g. 17th LBS, compare stages 4.2 and 5). Overall, the maturation of the germ band is characterised by the condensation of segment primordia towards the anterior, accompanied by the condensation of cells from the lateral parts of the posterior disc towards the midline.

The duration and rate of development

Fig. 8 shows a schematic representation of the stages previously described on a timeline for *Strigamia* development, with the duration of stages expressed as a percentage of development, based on our analysis at 13 °C.

The overall duration of development at 13 °C is about 48 days, from egg lay to hatching. There is some egg-to-egg variation, and this may be considerable for eggs that have been handled for observation and subjected to transient temperature or osmotic shocks. The synchrony of eggs within a given clutch is best for eggs that are left undisturbed at a constant temperature. Under these conditions, eggs of a single clutch frequently hatch within 48 h (i.e. approx. 5% developmental time). We do not know to what extent this reflects variation in the rate of development, rather than variation in the time of egg activation during laying.

The duration of development is highly temperature dependent—at 10–11 °C, development takes about 1/3 longer than at 13 °C (approx. 64 days). Comparison of the relative duration of stages at 10 and 13 °C reveals no great difference in the relative duration of early (stages 1–3), segmentation (stages 4–6) and later (stages 7–8) development (data not shown). We do not have complete developmental

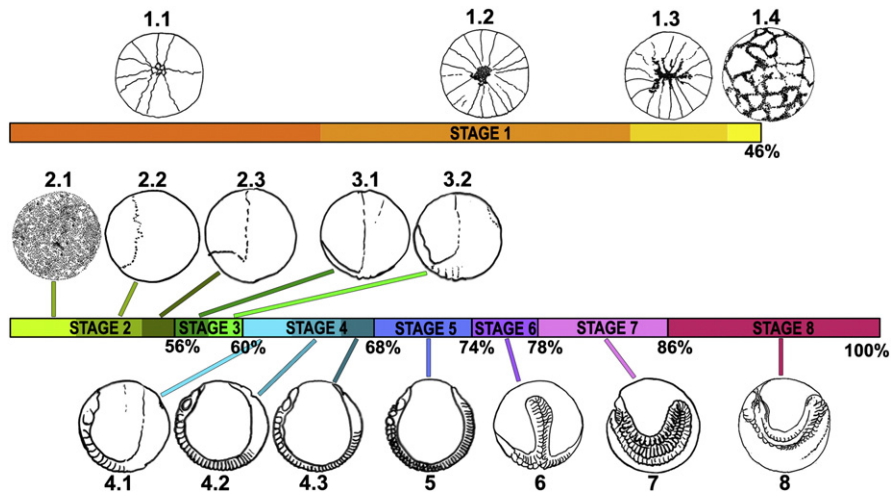


Fig. 8. Schematic representation of *Strigamia* development: *S. maritima* development is represented by a series of schematic drawings (traced from photographs) exemplifying each stage (stages 1.1 to stage 8). Bars are scaled to represent the duration of each developmental stage. Different colours represent different major stages, different tones of the same colour represent subdivisions of each major stage. The approximate cumulative percentage of the overall developmental period at the end of each stage is indicated.

data for higher temperatures, but at 20 °C, the second half of development, from germ band flexure to hatching, takes less than half of the time at 13 °C.

A striking feature of the developmental timeline is the prolonged duration of early cleavage (stage 1), which takes almost half of the total period of embryogenesis (46% of development). The following phase of blastoderm development and head condensation (stage 2) is also rather slow, accounting for 10% of developmental time.

In contrast, the process of segment generation is rather rapid. Patterning of the head and the first five visible segments happens within 4% of development, (stage 3) and then after a short pause (see above), the bulk of the remaining trunk segments (LBS 2–40) appear during stage 4, which occupies only 8% of development. The final few leg-bearing segments are added more slowly, before and after the dramatic movements of germ band flexure. Most overt differentiation and organogenesis occurs after flexure, in the final 20–25% of development.

The rate of segment formation

The first 5 ‘morphological’ segments (mandibular to 1st LBS: stage 3) are not easy to identify in live eggs as they appear during stage 3. Molecular data suggest that they appear in sequence (Chipman et al., 2004b and data not shown), but we do not have a precise timing for the appearance of these segments.

For the following stages, though, we have a set of 30 eggs raised at 13 °C whose leg-bearing segment number has been recorded daily from the beginning of stage 4 to hatching, by which time furrows demarcating the final adult number of leg-bearing segments are evident. Fig. 9 shows the averaged count of segment number for these eggs each day, and the counts for a single representative individual from this set. Data were collected according to method 2 as described in the Materials and methods.

We can define three phases of trunk segment addition. Throughout stage 4, segments, defined by morphological furrows, are added at a uniform rate of about 1 segment every 3.2 h (at 13 °C) up to around 38–40 LBS. The addition of segments then slows to 1–2 per day during stage 5, and stops during stage 6 for a couple of days while dorso-ventral flexure drastically repositions the whole embryo. Segmentation then restarts with a more or less linear pace of 1 seg/day during stage 7 and stage 8. We do not know the time of formation of the furrow defining the posterior of the last leg-bearing segment, because this appears after apolysis of the embryonic cuticle, and is not recognisable externally until after hatching.

We have also followed the appearance of segments up to sinking in embryos raised at 10–11 °C. Total visible segment number was counted at least daily for a cohort of 28 eggs from two clutches, and the developmental staging of all eggs was normalised by setting the time of mid-flexure of each egg to 0 (see Materials and methods). The rate of segment addition during stage 4 estimated from these data is 4.0 h/segment. Limited data suggest that the rate of segment formation at 8 °C is about 1 segment every 8 h, while at 20 °C it is close to 1 segment every hour (data not shown).

Discussion

The information provided in this paper provides a basis for detailed studies of early development and patterning in one of the few non-insect arthropods for which good genomic tools are also available. As a model *S. maritima* is far from perfect, but among the myriapods it is one of the best available for descriptive molecular embryology, and

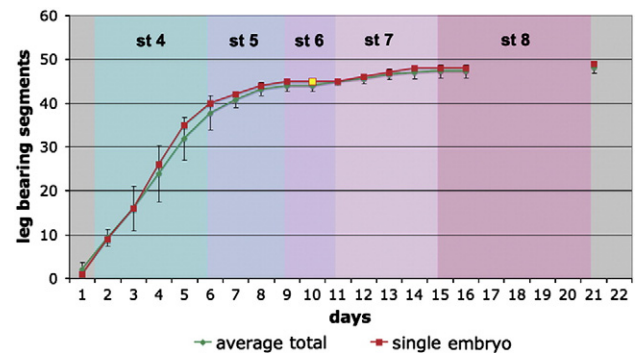


Fig. 9. Rate of addition of leg-bearing segments in *Strigamia* through stages 4–8 of development. Plots show the segment number each day for a single embryo (red) and for the average of 30 embryos (green). The data have been aligned at stage 6 as described in the Materials and methods. Error bars show the standard deviation of the samples at each time point. Segments are added at an almost constant rate up to around 38–40 LBS. After that, segmentation slows, and pauses completely during stage 6 (highlighted in yellow, dorsoventral flexure), before continuing slowly in the following stages. Note that segment addition cannot be monitored in live embryos during stage 8. The final isolated point is the segment number at hatching. The single specimen plotted here is that illustrated in Figs. 6a, b, c, f, g, i, l. Background colours mark the duration of stages 4 to 8 (st4 to st8).

there is considerable scope for the further development of manipulative tools. It is well placed to contribute to our understanding of the evolution of such developmental processes as axial patterning, mesoderm formation and segmentation, allowing polarisation of character states unique to clades within the Pancrustacea, and providing an important data point for the inference of traits ancestral to the arthropods as a whole.

The primary limitations of the system are probably those of the breeding system and lifecycle (see below). It should also be recognised that geophilomorph centipedes are a derived clade within the myriapods, exhibiting particularly high segment numbers and epimorphic development, i.e. attaining final segment number during embryogenesis (Edgecombe and Giribet, 2007). With the exception of scolopendromorphs, all other myriapods are anamorphic, adding segments progressively after hatching. Neither of these traits is ancestral to the centipedes, let alone the myriapods. While this argues for caution in making evolutionary comparisons, it also makes *Strigamia* particularly convenient to study the process of segmentation itself, and geophilomorphs interesting as a system to study inter and intraspecific variability of segment numbers. Among the geophilomorphs, *Strigamia* is currently uniquely tractable.

Strigamia as a system for developmental study

There is no truly convenient laboratory model among the centipedes. The few species that have been used for molecular developmental study in recent years (*S. maritima* and *Lithobius* species) are temperate species that have seasonal breeding and life cycles of more than a year. None of these has yet been maintained as permanent breeding colonies. Eggs have generally been collected from wild caught specimens, or, as in the case of *Strigamia*, collected directly from the field. Captive bred centipedes are mostly large Scolopendromorph species that are kept as pets—but these are seriously venomous and also have long life cycles. It seems likely that the shortest lifecycles will be found among small tropical species, which are also most likely to show continuous breeding, but these have not yet been surveyed for species that might be suitable for laboratory study.

S. maritima is exceptional in that its natural populations reach very high breeding densities in suitable environments. This allows us to collect tens of thousands of eggs for molecular and developmental study in just one or two days of field collection, without significantly affecting the natural population. We know of no other centipede for which this would be feasible.

The limitation of seasonal breeding is a serious one for working with live embryos. We can to some extent extend the availability of embryos for experiment by keeping the early eggs at 4 °C, but extending this beyond a few weeks leads to an increasing fraction of inviable eggs and abnormal embryos.

The tempo of early Strigamia development

The process of embryonic development in *Strigamia* is prolonged—48 days at our standard temperature of 13 °C, a temperature chosen as close to the average temperature that we have measured at the brooding sites when we collect the eggs. Development can progress very slowly at 4 °C, and is substantially faster at 20 °C, the maximum temperature that we have ever recorded at a natural breeding site in Brora (in 2011). This appears to be close to the maximum temperature that the Brora population will tolerate. At 25 °C, many eggs from this population do not develop normally. We do not know if populations from southern parts of the species range are more tolerant of these high temperatures.

One reason for the extended period of embryogenesis is the very long duration of the cleavage stage (22 days at 13 °C). For comparison, insect embryos frequently complete cleavage at 10–20% of development (Bentley et al., 1979; Foe and Alberts, 1983). During this time

the centipede embryo generates a population of many tens of thousands of cells, considerably larger than would be typical in an insect embryo at the same stage. Subsequent development proceeds with larger cell populations than would be typical for patterning in insect and crustacean embryos, which make embryos with initially as few as four cell rows per segment. In *Strigamia*, segments are generated with 6 or more rows of cells/segment, despite the large number of segments to be generated.

The nature of initial cleavage

A process of cleavage and cell migration similar to that we observe in *Strigamia* has been described in other Epimorpha centipedes (i.e. Scolopendromorpha, Heymons, 1901, and Geophilomorpha, Sograff, 1883).

One unresolved question concerns the nature of the early cleavages. We do not have data on the initial steps of egg maturation and fertilisation of the oocyte nucleus, but it is clear that the first divisions of the zygote nucleus take place at the centre of the egg, and that at about the same time as these first cleavages, the yolk becomes divided into discrete segments called yolk pyramids. Sograff (1883), also working with a geophilomorph centipede, interpreted the yolk pyramids as blastomeres generated by a complete initial cleavage. Heymons (1901) working with *Scolopendra*, also considered them to be of a cellular nature, but he could not identify an associated nucleus. Our observations that the yolk pyramids seem to have the first cell bodies at their internal apex, and that actin filaments extend along the margins of the yolk pyramids (Fig. 1), suggest to us that these pyramids may indeed be continuous with the first blastomeres. The matter is not yet fully resolved, but if this view is correct, then cleavage in geophilomorphs would be total, as in all other myriapods (Anderson, 1973), including the more basal centipede *Scutigera* (Knoll, 1974).

Whatever the nature of the first cleavages, it is clear that a population of yolk-free cells is quickly generated by subsequent divisions at the centre of the egg, and that the descendants of these cleavage cells migrate to the surface between the remaining yolk pyramids to form the blastoderm. This peculiar migration of cells from the centre of the egg to the surface is very different from the migration, not of cells but of energids, that is observed in spiders and insects, and which in insects generates the familiar syncytial blastoderm.

Blastoderm formation, gastrulation and the breaking of symmetry

Once at the surface, cells spread over the surface of the yolk to form a uniform, if initially somewhat irregular, monolayered blastoderm. Up until this stage, we have seen no indication of any consistent axial asymmetry in the egg or embryo.

At the very early blastoderm stages, we believe that there is a morphological marker that breaks symmetry—the appearance of a small multilayered cluster of cells visible at one point on the blastoderm surface. Unfortunately eggs at this stage are very difficult to dechorionate without damaging the blastoderm, and we have few good specimens, but all those that are reasonably complete show such a cluster.

The uniform blastoderm stage is brief. Almost as soon as cells have spread to make a monolayer, part of the surface becomes multilayered. This part is centred on a defined, circular region that remains monolayered (Fig. 2c), and also expresses *dpp* (Brena, unpublished data). We interpret this as being the blastopore. Continuity of morphology and of gene expression in a series of fixed embryos suggests that the blastopore forms adjacent to or incorporates the early cell cluster. The multilayered part of the blastoderm (MLB) initiates at this posterior focus, and spreads until it encompasses somewhat more than the whole posterior hemisphere of the egg.

The question of a cumulus in myriapods

An initial concentration of cells at one point in the blastoderm has been described in early stages of *Scutigera* (Knoll, 1974) and *Scolopendra* (Heymons, 1901) embryos among the centipedes, and a similar cluster is described in the diplopod *Glomeris* (Dohle, 1964). These “keimstelle”, or “cumulus primitivus” are thought to be associated with the formation of the blastopore, marking the future posterior of the embryo and associated with ingression/formation of the mesoderm.

The term “cumulus primitivus” has also been used in spiders to describe a thickening at the centre of the forming germinal disc, which marks the site where the blastopore will form (e.g. see Anderson, 1973). This has been called more recently also the “primitive plate”, “anterior cumulus” and “primary thickening” (see Chaw et al., 2007). At the first appearance of this primary thickening, the embryo is radially symmetrical.

A small cluster of internalised mesenchymal cells migrates from this thickening towards the periphery of the germinal disc, thereby defining the major axis of the embryo (Akiyama-Oda and Oda, 2003, 2006). These cells, termed the “cumulus posterior” when first described (see Anderson, 1973), but often referred to simply as the cumulus, particularly in recent papers (Akiyama-Oda and Oda, 2003; McGregor et al., 2008), have been shown to serve as a signalling centre, secreting dpp. They come to lie posterior to the caudal lobe of the embryo, and disappear as the germ band forms.

In one Scolopendromorph species, a cell cluster, possibly in continuity with the initial “cellular mass”, migrates further posteriorly at germ band stages before disappearing (Sakuma and Machida, 2002, 2003). This behaviour has led to the suggestion of a parallel between this cell cluster and the “cumulus posterior” of spiders. We have seen no clear evidence for such a posteriorly migrating cell cluster in *Strigamia*. At present we do not think that it is possible to draw any firm conclusion regarding the relationship between the early cell clusters of myriapod embryos, the later cell cluster described by Sakuma and Machida, and the cumulus posterior of spiders (cf. Mayer and Whittington, 2009).

Germ band dynamics

The germ band takes shape not only through condensation of the widely extended MLB, but also through extension in two directions. The anterior margin of the head condensation moves forwards over the underlying yolk, while the proctodeum, which first becomes apparent close to the centre of the MLB as the blastopore, moves in the opposite direction, approaching the posterior margin of the shrinking posterior disc. At the same time, as the germ band matures, the anterior segments initially formed condense to occupy a smaller fraction of the germ band, as more segments are added at the posterior. It is essential to appreciate these movements in order to understand the relation between tissue movement and changes in gene expression patterns during germ band elongation.

An initial elongation of the germ band seems to be associated only with those centipedes that develop epimorphically and hatch as long bodied forms, i.e. the Scolopendromorpha and Geophilomorpha. It is not present, at least once segmentation has started, in anamorphic centipedes like *Lithobius* or *Scutigera*, (Kadner and Stollewerk, 2004; Knoll, 1974) or in diplopods like *Glomeris* (Dohle, 1974), that hatch as short bodied forms (hatching with only 7, 4 and 3 pair of legs, respectively).

The dorso ventral flexure

A dramatic lateral spreading, accompanied with dorso-ventral flexure of the germ band, is observed in many terrestrial non-insect arthropods. It is present in most myriapods (with the exception of the miniaturised *Pauropus*), and also in spiders, where it is referred to as

inversion (Anderson, 1973). However, there is a significant difference in the process of lateral spreading as we see it in *Strigamia*, from that reported in Scolopendromorphs (Heymons, 1901; Whittington et al., 1991). We find that the neural tissue remains medial in *Strigamia*, with an attenuated membrane interposed between these medial tissues and the lateral/dorsal parts of the segments bearing the limb buds and tergites. In Scolopendromorphs, the neurectoderm moves laterally, with the initial spreading happening between the left and right halves of the nervous system. Only later, does the nervous system become separated from the lateral/dorsal parts of the segment, as in *Strigamia* (Heymons, 1901; Whittington et al., 1991). In spiders, the nervous system is also split during lateral spreading (Stollewerk et al., 2001).

Segmentation

In the *Strigamia* embryo, most segments are first demarcated morphologically by transverse furrows that extend across the complete width of the germ band, and only later by the appearance of distinct limb buds. This applies to the mandibular, and all more posterior segments. *Engrailed* staining appears shortly (1–2 segments) ahead of these furrows (Chipman et al., 2004b; Kettle et al., 2003 and data not shown).

Segments in the more anterior part of the head are not defined by such furrows. The antennal segment becomes visible as the antennal lobes themselves are defined. *Engrailed* is only ever expressed as two lateral stripes in the region of the lobes. The intercalary segment, although clearly defined by engrailed and other molecular markers (Chipman and Akam, 2008; Chipman and Stollewerk, 2006; Chipman et al., 2004b), is never visible morphologically at any stage of development. The ocular region, sometimes considered to be a distinct segment, is demarcated only by a bulging outline in this part of the head condensation. It shows no early *engrailed* expression in *Strigamia*. There is thus, from the very beginning, a clear difference between the anterior part of the head (procephalon) and all the following segments. The ‘segments’ we refer to in the following discussion on segmentation are exclusively the post-intercalary segments.

Strigamia is an example of short germ development, in the sense that segments appear strictly sequentially from anterior to posterior along the AP axis. However, this mode of development differs from short germ insect development as defined by Sander (1976), in that, at the onset of segment addition, the posterior part of the embryo is represented by a large population of cells, and not just by a small growth zone. For this reason, we prefer to refer to the *Strigamia* embryo as sequentially segmenting, rather than short germ (Peel et al., 2005).

We subdivide the process of segment addition into 4 distinct phases, based on the dynamics of the process, although we do not thereby imply that each of these phases uses different molecular machinery.

5 segments form in the first phase (stage 3.1) – the 3 mouthpart segments, the forcipular or maxillipedal segment and the 1st LBS. Segment addition pauses briefly at this point (stage 3.2). From the distribution of stages in fixed clutches, and the frequency of “5-segment” embryos in larger batches of fixed embryos, this pause is equivalent to the time it takes to make five or more trunk segments.

The pause between the formation of these 5 most anterior segments and those of the rest of the trunk is reminiscent of the pause between the formation of the prosomal segments in spiders, which appear almost simultaneously, and the addition of opisthosomal segments sequentially in a second phase (Gilbert, 1997). It also parallels the formation of the most anterior segments before hatching in diplopods (up to the 3rd LBS in most of them) and the addition of the following segments post-embryonically (Dohle, 1974). If the expression patterns of Hox and other genes are a good guide to segment homology (Damen et al., 1998; Telford and Thomas, 1998), these ‘anterior segment’ regions do not

correspond precisely in the different groups (the last prosomal segment of spiders is homologous to the maxilliped of centipedes, and the 3rd LBS of *Glomeris* is homologous to the 2nd LBS of centipedes). However, a difference in the patterning of anterior and posterior segments may be a common feature of arthropods.

During the second phase of segment addition (stage 4), most trunk segments are added at a constant rate: ≈ 1 seg every 3.2 h at 13 °C. Mitoses are frequently observed in the posterior disc at this stage, suggesting that cells are still dividing during this period, but clearly they are not proliferating fast enough to keep up with the withdrawal of cells into formed segments. (Note that the whole of stage 4 is less than one fifth the duration of the period of cleavage prior to blastoderm formation, so in terms of cell cycles, it is likely that most cell divisions happen before trunk segmentation starts). The segmentation front approaches progressively closer to the proctodeum as segmentation proceeds, reducing yet further the 'growth zone' within which proliferation can generate cells for new segments. It may be at least in part for this reason that the rate of segmentation slows progressively after about the 38 LBS to a rate of one or two segments per day (phase 3 of segmentation, stage 5). There are likely other controls too, as segment addition stops completely during the process of germ band flexure (stage 6), only to start again at a similar slow rate (about 1 segment/day) once flexure is complete (phase 4 of segmentation, stages 7 and 8).

Embryonic vs post-embryonic segmentation

Scolopendromorph and geophilomorph centipedes make all their leg-bearing segments embryonically, even though they have the highest number of segments of any centipedes (up to 191 LBS in geophilomorphs). Indeed, it is the determination of the final segment number in the embryo, and the intra-specific variability of the same, that make the geophilomorph centipedes so interesting as models for segmentation from both a developmental and evolutionary point of view.

This character, used to group these two orders in the clade Epimorpha, is clearly derived within the Myriapoda, given that all other groups are anamorphic, adding segments post-embryonically. In anamorphic groups, segments develop under the cuticle, at the posterior end of the animal, just anterior to the proctodaeal area, and at each moult the animal comes out of the exuvia with more segments. The similarity with the final stages of embryonic segmentation in *Strigamia* is now clear. We find that the posterior furrow defining the last leg-bearing segment in *Strigamia* appears after apolysis of the embryonic cuticle, and hence, developmentally, can be considered to form during the first larval instar. The addition of this last segment pair appears to be the last remnant of the post-embryonic segmentation that probably characterised the ancestor of the epimorphic groups.

Supplementary materials related to this article can be found online at doi:10.1016/j.ydbio.2011.11.006.

Acknowledgements

This work was funded by the BBSRC grant No. BBS/B/07519 to MEA, and by the University of Cambridge VIP fund. We thank Alessandro Minelli for assistance in obtaining obscure references, Matt Benton for providing Fig. S3 and to all members of the Akam and Arthur labs who have participated in the field collection of *Strigamia* embryos.

References

- Akiyama-Oda, Y., Oda, H., 2003. Early patterning of the spider embryo: a cluster of mesenchymal cells at the cumulus produces Dpp signals received by germ disc epithelial cells. *Development* 130, 1735–1747.
- Akiyama-Oda, Y., Oda, H., 2006. Axis specification in the spider embryo: dpp is required for radial-to-axial symmetry transformation and sog for ventral patterning. *Development* 133, 2347–2357.
- Anderson, D.T., 1973. *Embryology and phylogeny in annelids and arthropods*. Pergamon Press, Oxford.
- Bentley, D., Keshishian, H., Shankland, M., Toroian-Raymond, A., 1979. Quantitative staging of embryonic-development of the grasshopper, *Schistocerca nitens*. *J. Embryol. Exp. Morphol.* 54, 47–74.
- Chaw, R.C., Vance, E., Black, S.D., 2007. Gastrulation in the spider *Zygiella x-notata* involves three distinct phases of cell internalization. *Dev. Dyn.* 236, 3484–3495.
- Chipman, A.D., Akam, M., 2008. The segmentation cascade in the centipede *Strigamia maritima*: involvement of the notch pathway and pair-rule gene homologues. *Dev. Biol.* 319, 160–169.
- Chipman, A.D., Stollewerk, A., 2006. Specification of neural precursor identity in the geophilomorph centipede *Strigamia maritima*. *Dev. Biol.* 290, 337–350.
- Chipman, A.D., Arthur, W., Akam, M., 2004a. A double segment periodicity underlies segment generation in centipede development. *Curr. Biol.* 14, 1250–1255.
- Chipman, A.D., Arthur, W., Akam, M., 2004b. Early development and segment formation in the centipede, *Strigamia maritima* (Geophilomorpha). *Evol. Dev.* 6, 78–89.
- Damen, W.G.M., Hausdorf, M., Seyfarth, E.A., Tautz, D., 1998. A conserved mode of head segmentation in arthropods revealed by the expression pattern of Hox genes in a spider. *Proc. Natl. Acad. Sci. U. S. A.* 95, 10665–10670.
- Dawydoff, C., 1956. Quelques observations sur l'embryogenese des Myriopodes Scolopendromorphes et Geophilomorphes Indochinois. *C. R. Hebd. Seances Acad. Sci.* 242, 2265–2267.
- Dohle, W., 1964. Die Embryonalentwicklung von *Glomeris marginata* (Villers) im Vergleich zur Entwicklung anderer Diplopoden. *Zool. Jb. Anat.* Bd. 81, 241–310.
- Dohle, W., 1970. Über Eiablage und Entwicklung von *Scutigera coleoptrata* (Chilopoda). *Bull. Mus. Hist. Nat. Paris* 41, 53–57.
- Dohle, W., 1974. The segmentation of the germ band of Diplopoda compared with other classes of arthropods. *Symp. Zool. Soc. Lond.* 32, 143–161.
- Edgecombe, G.D., Giribet, G., 2007. Evolutionary biology of centipedes (Myriapoda: Chilopoda). *Annu. Rev. Entomol.* 52, 151–170.
- Foe, V.E., Alberts, B.M., 1983. Studies of nuclear and cytoplasmic behavior during the 5 mitotic-cycles that precede gastrulation in *Drosophila* embryogenesis. *J. Cell Sci.* 61, 31–70.
- Gilbert, S.F., 1997. Arthropods: crustaceans, spiders, and myriapods. In: Gilbert, S.F., Raunio, A.M. (Eds.), *Embryology: Constructing the Organism*. Sinauer Associates, Sunderland, MA, pp. 239–257.
- Hertzel, G., 1983. Cuticuläre Hüllen in der Embryogenese von *Lithobius forficatus* (L.) (Myriapoda, Chilopoda). *Zool. Jb. Anat.* 110, 395–401.
- Hertzel, G., 1984. The segmentation of the germ band of *Lithobius forficatus* (Myriapoda, Chilopoda). *Zool. Jb. Anat.* 112, 369–386.
- Heymons, R., 1898. Bemerkungen zu dem Aufsatz Verhoeff's "Noch einige Worte über Segmentanhänge bei Insekten und Myriopoden". *Zool. Anz.* 21, 173–180.
- Heymons, R., 1901. Die Entwicklungsgeschichte der Scolopender. *Zoologica* (Stuttgart) 13, 1–244.
- Ho, K., DuninBorowski, O.M., Akam, M., 1997. Cellularization in locust embryos occurs before blastoderm formation. *Development* 124, 2761–2768.
- Ivanov, P.P., 1940. Embryonic development of *Scolopendra* with reference to the embryology and morphology of Tracheata. *Izv. Akad. Nauk SSSR* 831–861.
- Johannsen, O.A., Butt, F.H., 1941. *Embryology of Insects and Myriapods*. McGraw-Hill, NY.
- Kadner, D., Stollewerk, A., 2004. Neurogenesis in the chilopod *Lithobius forficatus* suggests more similarities to chelicerates than to insects. *Dev. Genes Evol.* 214, 367–379.
- Kettle, C., Johnstone, J., Jowett, T., Arthur, H., Arthur, W., 2003. The pattern of segment formation, as revealed by engrailed expression, in a centipede with a variable number of segments. *Evol. Dev.* 5, 198–207.
- Knoll, H.J., 1974. Untersuchungen zur Entwicklungsgeschichte von *Scutigera coleoptrata* L. (Chilopoda). *Zool. Jb. Anat.* Bd. 92, 47–132.
- Lewis, J.G.E., 1961. The life history and ecology of the littoral centipede *Strigamia* (= *Scolioptanes*) *maritima* (Leach). *Proc. Zool. Soc. Lond.* 137, 221–248.
- Mayer, G., Whittington, P.M., 2009. Velvet worm development links myriapods with chelicerates. *Proc. R. Soc. B* 276, 3571–3579.
- McGregor, A.P., Hilbrant, M., Pechmann, M., Schwager, E.E., Prpic, N.M., Damen, W.G.M., 2008. *Cupiennius salei* and *Achaearanea tepidariorum*: spider models for investigating evolution and development. *Bioessays* 30, 487–498.
- Metschnikoff, E., 1875. Embryologische über Geophilus. *Z. Wiss. Zool.* 25, 312–322.
- Peel, A.D., Chipman, A.D., Akam, M., 2005. Arthropod segmentation: beyond the *Drosophila* paradigm. *Nat. Rev. Genet.* 6, 905–916.
- Sakuma, M., Machida, R., 2002. Germ band formation of the centipede *Scolopocryptops rubiginosus* L. Koch (Chilopoda: Scolopendromorpha). *Proc. Arthropod. Embryol. Soc. Jpn.* 37, 19–23.
- Sakuma, M., Machida, R., 2003. "Cumulus posterior"-like structure in the centipede *Scolopocryptops rubiginosus* L. Koch (Chilopoda: Scolopendromorpha). *Proc. Arthropod. Embryol. Soc. Jpn.* 38, 37–39.
- Sakuma, M., Machida, R., 2004. Germ band formation of the centipede *Scolopendra subspinipes* L. Koch (Chilopoda: Scolopendromorpha). *Proc. Arthropod. Embryol. Soc. Jpn.* 39, 41–43.
- Sakuma, M., Machida, R., 2005. Clypeolabrum formation of a centipede *Scolopocryptops rubiginosus* L. Koch (Chilopoda: Scolopendromorpha). *Proc. Arthropod. Embryol. Soc. Jpn.* 40, 1–4.
- Sander, K., 1976. Specification of the basic body pattern in insect embryogenesis. *Adv. Insect Physiol.* 12, 125–238.
- Sograff, N., 1882. Zur Embryologie der Chilopoden. *Zool. Anz.* 5, 582–585.
- Sograff, N., 1883. Materialien zur Kenntnis der Embryonalentwicklung von *Geophilus ferrugineus* L. K. und *Geophilus proximus* L. K. *Nachricht. Ges. Freunde Naturkunde, Anthropol. Ethnolog., Moskau* 43, 1–77.
- Stollewerk, A., Weller, M., Tautz, D., 2001. Neurogenesis in the spider *Cupiennius salei*. *Development* 128, 2673–2688.
- Telford, M.J., Thomas, R.H., 1998. Expression of homeobox genes shows chelicerate arthropods retain their deutocerebral segment. *Proc. Natl. Acad. Sci. U. S. A.* 95, 10671–10675.

- Vedel, V., Chipman, A.D., Akam, M., Arthur, W., 2008. Temperature-dependent plasticity of segment number in an arthropod species: the centipede *Strigamia maritima*. *Evol. Dev.* 10, 487–492.
- Vedel, V., Brena, C., Arthur, W., 2009. Demonstration of a heritable component of the variation in segment number in the centipede *Strigamia maritima*. *Evol. Dev.* 11, 434–440.
- Vedel, V., Apostolou, Z., Arthur, W., Akam, M., Brena, C., 2010. An early temperature-sensitive period for the plasticity of segment number in the centipede *Strigamia maritima*. *Evol. Dev.* 12, 347–352.
- Whittington, P.M., Meier, T., King, P., 1991. Segmentation, neurogenesis and formation of early axonal pathways in the centipede, *Ethmostigmus rubripes* (Brandt). *Roux' Arch. Dev. Biol.* 199, 349–363.